

**Reconstruction of the Cretaceous and Paleogene  
Lithostratigraphy of the Fergana Basin, Uzbekistan:  
Paleoenvironmental Change Related with the Development of  
the proto-Paratethys Sea**

July 2022

ANVAROV OTABEK ULUGBEK OGLI

**Reconstruction of the Cretaceous and Paleogene  
Lithostratigraphy of the Fergana Basin, Uzbekistan:  
Paleoenvironmental Change Related with the Development of  
the proto-Paratethys Sea**

A Dissertation Submitted to  
the Graduate School of Life and Environmental Sciences,  
the University of Tsukuba  
in Partial Fulfillment of the Requirements  
for the Degree of Doctor of Philosophy in Science  
(Doctoral Program in Earth Evolution Sciences)

ANVAROV OTABEK ULUGBEK OGLI

## **Contents:**

Contents .....	i
Abstract .....	iv
List of Figures .....	vi
List of Tables .....	viii

## **Chapter I: The Cretaceous system distributed in the Fergana Basin and Dzharakuduk, Kyzylkum Desert, Uzbekistan**

1. Introduction .....	1
1.1. General Geographical Outlines of Uzbekistan .....	1
1.2. General Geological Outlines of Uzbekistan .....	4
1.2.1. Precambrian rocks .....	5
1.2.2. Paleozoic rocks .....	7
1.2.3. Mesozoic rocks .....	11
1.2.4. Cenozoic rocks and sediments .....	12
1.3. The Cretaceous System of Uzbekistan .....	13
1.4. The purpose and aims of the study .....	16
2. The Cretaceous of the Fergana Basin and Dzharakuduk Site: Lithostratigraphy and Vertebrate Fossils .....	17
2.1. The Cretaceous Sequences of the Fergana Basin .....	17
2.2 Description of the observed sections in Gava and Varzyk area, northern Fergana Basin.....	23
2.3. The Cretaceous Sequences Vertabrate Fossils in Dzharakuduk Site .....	29

3. Discussion .....	39
4. Conclusion .....	41

**Chapter II: The Fourth Marine Incursion of paleo-Paratethys in the Northern Fergana Basin**

1. Introduction .....	43
2. Geological Outlines of the Paleogene Northern Fergana Basin .....	48
2.1. Limestone-clastic sequence in the northwestern Fergana Basin .....	50
2.1.1. Karabulak Section .....	52
2.1.2. Varzyk Section .....	56
2.1.3. Gava 1 and Gava 2 Sections .....	58
3. Methods .....	61
3.1. Sampling and preparation for isotope measurements .....	61
3.2. Fossil Identification .....	65
3.3. Stable Isotope Analysis .....	68
3.3.1. Sulfur isotope analysis of the BaSO <sub>4</sub> precipitates of the carbonate – associate sulfate .....	68
3.3.2. Strontium isotope analysis .....	70
4. Results .....	71
5. Discussions .....	73
5.1. Stratigraphy .....	73
5.2. Geochronology .....	76
5.3. The Fourth Marine Incursion of the paleo-Paratethys .....	81
6. Conclusions .....	83

Acknowledgements .....	85
References .....	89

## **ABSTRACT**

The Fergana Basin which is in the eastern part of the Republic of Uzbekistan, Central Asia has a unique importance in both geological and resources aspects. The history of the studies about the basin dates back to the end of the 19th century by Russian scientists. Because of the rich resources, the interest in research related to the geology of the basin increased from the 1930s to the 50s of the 20th century as it was colonized by the Soviet Union. There was little research after the independence of Uzbekistan, but it was not introduced to the world. Therefore, this doctoral research is dedicated to the introduction of the geology of not only the Fergana Basin but also the geology of Uzbekistan.

The aim of this research is to establish the lithostratigraphy of the Cretaceous and the Paleogene of the Fergana Basin with not only the field observation but also the methods such as stable isotope analysis which was used for the first time in the geological research of the basin.

The first chapter focuses on sedimentary rocks of Cretaceous distributed on basins of the Republic of Uzbekistan, and geological correlation between the Cretaceous sedimentary rocks of the Kyzylkum region where dinosaur fossils had been reported recently and that of the Fergana basin. In this chapter, not only the Cretaceous period but also the general geology of the Republic of Uzbekistan will be introduced. As noted above most of the previous research was in Russian, therefore this chapter will be a review of the correlations to the new lithostratigraphic data which was obtained from the northern part of the Fergana Basin. The most important point is the geological correlation between the Cretaceous Formation distributed in the Kyzylkum Desert which is famous for its diverse fossil content and that of the Fergana Basin.

The second chapter will address to Paleogene period of the Fergana Basin. The lithostratigraphy and isotopic compositions of the Paleogene sequences consisting mainly of terrestrial clastics with limestone were examined in the northern part of the Fergana Basin. Altogether four sections were studied at three localities near the Chust city, Namangan Region. The studied sequences consist of two facies: coarse-grained terrestrial clastics in the lower section and limestone-clastic sequences characterized by intercalated limestone beds in the upper section. The results showed that the sulfur isotopic composition of the bivalve yielding from the lower sequence has a lower composition of 14.94–16.82 ‰. This isotopic composition is equivalent to that of the Early Cretaceous; however, it is possible that the isotope composition recorded different values from open seawater by terrestrial clastics and freshwater effect, and therefore this lower section was also mentioned in the first chapter. The sulfur isotope value of the limestones consisting of the limestone–clastic sequence indicates a higher composition of 19.37‰–21.19‰, and it is likely that the limestones were assigned to be in the early Eocene. On the other hand, the strontium isotope compositions of the lower and upper sequences were 0.707772–0.707875 and 0.707812–0.708063, respectively. These values are more like those of the Paleogene than those of the Cretaceous. The lithostratigraphy and age determination allowed to correlate the upper limestone-clastic sequence with representative limestone of the fourth transgression of the proto-Paratethys Sea. Therefore, in a conclusion, the limestone beds are considered as the remnants of the Eocene marine incursion of the proto-Paratethys.

*Keywords:* Cretaceous, Fergana Basin, Kyzylkum Desert, proto-Paratethys Sea, stable isotopic composition, strontium, sulfur, Paleogene, Uzbekistan.

## List of Figures

### Chapter I: The Cretaceous system distributed in the Fergana Basin and

#### Dzharakuduk Site of the Republic of Uzbekistan

Figure 1. The location map of the Republic of Uzbekistan .....	2
Figure 2. Geological map of the Republic of Uzbekistan .....	6
Figure 3. Distribution of the Cretaceous deposits in the Republic of Uzbekistan .....	14
Figure 4. Location and geological map of the Fergana Basin .....	18
Figure 5. Location of the study area, Northern part of the Fergana Basin .....	24
Figure 6. Columnar cross-sections of this study Gava Section .....	25
Figure 7. Representative photographs from Gava Section .....	26
Figure 8. Columnar cross-sections of this study Varzyk Section .....	27
Figure 9. Representative photographs from Varzyk Section .....	28
Figure 10. Location map of the Kyzylkum Desert and Dzharakuduk Site .....	30
Figure 11. The representative photographs of the canyons and cliffs of the Dzharakuduk Site .....	31
Figure 12. The specimen of the newly discovered carcharodontosaurian theropod dinosaur <i>Ulugbegsaurus uzbekistanensis</i> and its illustration .....	38
Figure 13. The lithological correlations of the Dzharakuduk Site and Fergana Basin, Varzyk Section .....	40



**Chapter II: The Fourth Marine Incursion of paleo-Paratethys in the Northern  
Fergana Basin**

Figure 1. The index and geological map of the Fergana Basin .....	45
Figure 2. The geological map of the northern part of the Fergana Basin .....	47
Figure 3. The columnar sections of the study area .....	51
Figure 4. The field photographs of the sedimentary rocks at the Karabulak Section .....	54
Figure 5. The field photographs of the sedimentary rocks at the Karabulak Section (continued) .....	55
Figure 6. The field photographs of the sedimentary rocks at the Varzyk Section .....	57
Figure 7. The field photographs of the sedimentary rocks at the Gava Section .....	59
Figure 8. Photomicrographs of the limestone and clastic sedimentary rocks from study section .....	60
Figure 9. The photographs of the sample preparation for isotope measurements .....	64
Figure 10. Macrofossil assemblage from upper sequence of the study area .....	66
Figure 11. Macrofossil assemblage from lower sequence of the study area .....	67
Figure 12. The LOWESS curve for sulfur and strontium for the last 130 Ma with isotopic compositions of current study .....	72
Figure 13. The illustration of the strontium isotope supply to the world oceans adopted by McArthur (1992) and modified to northern part of the Fergana Basin .....	80

## List of Tables

### Chapter I: The Cretaceous system distributed in the Fergana Basin and

#### Dzharakuduk Complex of the Republic of Uzbekistan

Table 1. List of the Paleozoic Formations of Uzbekistan (Cambrian, Ordovician and Silurian) .....	9
Table 2. List of the Paleozoic Formations of Uzbekistan (continued) (Devonian, Carboniferous and Permian) .....	10
Table 3. List of the Cretaceous Formations of the Republic of Uzbekistan .....	15
Table 4. The list of the Cretaceous Formations of the Fergana Basin .....	21
Table 5. The list of the Cretaceous Formations of the Kyzylkum Desert and Dzharakuduk Site .....	33

### Chapter II: The Fourth Marine IncurSION of paleo-Paratethys in the Northern

#### Fergana Basin

Table 1. The detailed table of the samples used for sulfur and strontium isotope analysis with observed isotope values .....	62
Table 2. The simplified correlation of the studied sections with adjacent Alai Valley Basin and Fergana Basin (Kyrgyzstan) .....	75

# **Chapter I: The Cretaceous System Distributed in the Fergana Basin and Dzharakuduk, Kyzylkum Desert Uzbekistan**

## **1. Introduction**

### *1.1. General Geographical Outlines of Uzbekistan*

Uzbekistan is located in Central Asia (Figure 1), between the Amu Darya and Syr Darya rivers, in the temperate zone of deserts and borders with Kazakhstan in the north, Kyrgyzstan in the east and southeast, Tajikistan in the southeast, and Turkmenistan in the southwest. In the south, in a small area along the Amu Darya River, there is a border with Afghanistan. The natural conditions of Uzbekistan are varied. According to the nature of the surface, the land of Uzbekistan is divided into two topographical parts: a large north-western part with a flat relief and a smaller south-eastern part, with foothills, and mountains.

The plains of Uzbekistan include most of the Kyzylkum desert with a wide development of eolian sands, the alluvial plain of the Amu Darya River, and the subaerial deltas of the Zeravshan and Kashkadarya rivers. The southeastern part of the Ustyurt plateau, which is an undulating plain with drainless solonchak<sup>1</sup> (poorly drained pale grey soil) depressions. The plains are generally favorable for economic activity under the condition of irrigation, watering, and water supply and are the main resource for expanding irrigated lands and increasing the productivity of natural pastures.

---

<sup>1</sup> Solonchak – poorly drained pale grey soil (from Russian), widely distributed in Central Asian countries and Russia



**Figure 1.** The Location Map of The Republic of Uzbekistan (Britannica Encyclopedia)

The foothill and mountainous parts of Uzbekistan include the western foothills of the Tien Shan and the Gissar-Alay ranges. Between the ridges are located: the Fergana Basin, often called the Fergana Valley, the Golodniy Steppe, which is an alluvial and alluvial proluvial flat plain, the valleys of the Chirchik, Angren, and Keles rivers, the Zeravshan, Kitab-Shakhrisabz, Surkhandarya depressions, the axial parts of which are occupied by river valleys.

Desert-type soils are located in the flat part of Uzbekistan: desert sandy, gray to brown, takir<sup>2</sup> soils and solonchaks. The hydromorphic soils are developed along the river valleys and in the deltas of the Amu Darya, Zeravshan, and some other rivers. These soils are characterized by high carbonate content, low content of humus, and salinity. The foothill plains are occupied by light and typical gray soil, and the low mountains are occupied by dark gray soil. Above the low mountains, there is a belt of medium-altitude mountains, where brown and dark brown mountain forest soils are distinguished.

The interior of Uzbekistan is rich in mineral resources. In the subsoils of the flat part there is oil, gas, bentonite clays, limestones, gypsum, building sands, sodium sulfate and magnesium salts; in the foothill-mountain part: copper, lead, gold, tungsten, iron ore, mercury, coal, fluorspar, aluminum raw materials, marble, granite, cement and brick raw materials, graphite, table and potassium salts, building materials and so on. These fuel, energy and mineral resources, together with agricultural products, create the necessary basis for the comprehensive development of a diversified industry.

---

<sup>2</sup> Takir – soil relief widely distributed in Central Asia. It is usually formed in the shallow depressed areas with a result of drainage of mud after waterfall season.

## *1.2. General Geological Outlines of Uzbekistan*

One of the characteristic features of the geological structure of Uzbekistan is the presence of two mega-complexes of rocks within its boundaries. The lower one is represented by intensely deformed diverse sedimentary, igneous, and metamorphic rocks of the Precambrian and Paleozoic ages, while the upper one is represented by sedimentary sequences of the Mesozoic and Cenozoic. The rocks of the lower mega-complex compose the Tien Shan Mountain ranges (Southern and Middle Tien Shan), and the upper one, Mesozoic and Cenozoic deposits, are distributed in the plains, intermountain valleys and depressions (Figure 2).

### 1.2.1 Precambrian rocks

The oldest rocks represented in Precambrian complexes, and only the Proterozoic formations have been discovered in the Central part of the Kyzylkum Desert, Gissar Range in southwest (South Tien Shan), and Chatkal Range northeast (Middle Tien Shan) (Figure 2.). Among them, along with undivided Proterozoic deposits, the Middle–Upper and Upper Rhiphaean (lower Mesoproterozoic) sequences were established (Akhmedjanov *et al.*, 1967 and Abdullaev *et al.*, 1989).

A characteristic feature of the Proterozoic rocks is the transition (from old to young) from highly metamorphosed rocks (in the amphibolite and epidote-amphibolite facies) to moderate metamorphosed in the greenschist facies or weakly metamorphosed rocks. The moderately metamorphosed rocks mainly include Rhiphaean (lower Mesoproterozoic) rocks. Among the highly metamorphosed rocks, gneisses of various compositions, schists, amphibolites, quartzites, and marbles are extended and mainly distributed in Bukantau Mountains in Kyzylkum Desert and Northern Nurata Range central Uzbekistan (Figure 2)(Mikhaylov, 2016).

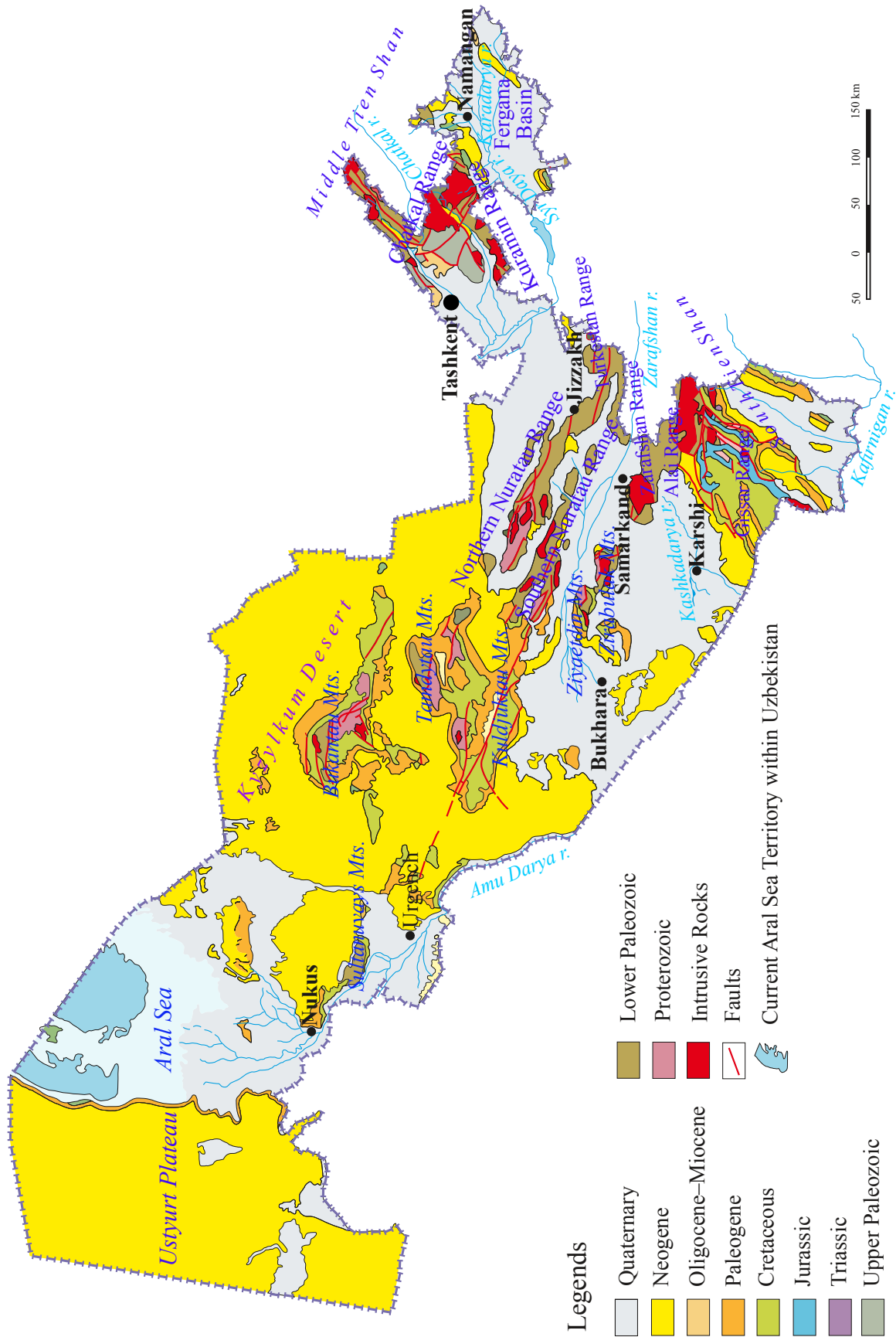


**Figure 2.** Geological Map of the Republic of Uzbekistan. Modified after Mirkamalov (2016) Atlas of Rep. of Uz.



### 1.2.2 Paleozoic rocks

The Paleozoic sedimentary rocks are widely distributed in Uzbekistan. However, the degree of their distribution over the land is all due to the individual history of the geological development. They distinguished from west to the east, and mainly the Paleozoic rocks are exposed in the central and eastern parts of Uzbekistan. This is due to the geological development of the Tien Shan mountains. (Zonenshain *et al.*, 1990).

According to Zonenshain *et al.* (1990) the Cambrian rocks are exposed only in the central Kyzylkum Bukantau (Khodjaahmet Fm.), Tamdytau (Kurgantau Fm.) and South Tien Shan mountains along the Zeravshan-Turkestan ranges (Altykol Fm.). The rocks are represented mainly terrestrial in the central part and marine in the southwest (Figure 2 and Table 1).

The Ordovician–Silurian deposits are represented by marine facies, terrestrial clastic and volcanogenic rocks, and these rocks are distributed mainly in the Nuratau and Tamdytau mountains, Central Uzbekistan. Both Lower and Upper Silurian sedimentary rocks were observed within the Southern and Middle Tien Shan (Kurenkov, 1983).

In general, the Ordovician and Silurian rocks throughout the Uzbekistan are represented complex lithology, i.e., among the terrestrial deposits not only clastic but also volcanogenic rocks are also represented and, in the formations, unified as terrestrial (Table 1). Only in Sultanuvays and Northern Tamdytau a terrigenous–volcanogenic rocks with basic and intermediate volcanic rocks were observed and the rest part were represented by marine and costal marine (Alai Range) (Mirkamalov *et al.*, 1991a, 1991b).

The Devonian sedimentary rocks are mainly preserved in the Middle and South Tien Shan and very well studied. Additionally, one of the three faunal stages of the Lower Devonian the Emsian of the Zinzil'ban Gorge, Gissar Range in the Kitab State Geological

Reserve got a golden spike of GSSP at the 9-5 section above the Madmon Formation. On all the ridges of the South Tien Shan, the Devonian system is mainly represented by marine and coastal-marine deposits. And only in the southern Fergana, the Devonian is composed of volcanogenic terrigenous formations (Mukhin *et al.*, 1989, Mikhaylov, 2016).

The Carboniferous sedimentary rocks are also widespread and mainly represented by marine sediments in the Central Kyzylkum and South Tien Shan. Both the Mississippian and the Pennsylvanian were observed in the Middle Tien Shan and northeastern Fergana Basin. But in the southwestern Tien Shan is represented by volcanogenic rocks (Chatkal and Kuramin ranges, Figure 2 and Table 2). The deposits of the Permian, in comparison with the Carboniferous, are much less common and are represented by the coastal and continental deposits. The Lower Permian terrestrial and carbonate deposits, in places containing volcanoes, are exposed in the South Fergana region of the South Tien Shan (Akhmedjanov *et al.*, 1967).

Era	Period	GTS		Paleozoic Formations of Uzbekistan											
		Epoch	Age	Ustyurt and Central Kyzylkum			South Tien Shan			Middle Tien Shan					
				Sultanuvsy	Bukantau	Tamdytau	Kuldjuktay	Nuratau	Gissar Range	Zirabulak-Ziaetdin	Zerafshan-Turkestan	Alai Range	Chatkai Range	Kuramin Range	
Paleozoic	Silurian	Pridoli		Urusay Fm.			Bashgujukumdy Fm.	Bayram Fm.	Yaxtagan Fm.	Pyazi Fm.	Zeravshan-Turkestan				
		Ludlow		Djartas Fm.				Akkayak Fm.	Zorxok Fm.	Terikbaba Fm.	Padask Fm.	Isfara Fm.			
		Wenlock					Djangleidy Fm.	Dzyush Fm.	Nofin Fm.	Makrid Fm.	Kuturaksay Fm.				
								Vaush Fm.	Machetili Fm.	Katadjar Fm.	Dugaba Fm.	Pulgon Fm.			
	Ordovician	Llandovery			Baymen Fm.			Ushkuduk Fm.	Djazbulak Fm.	Khokgaltak Fm.	Ovkhon Fm.	Guralash Fm.			
								Darbaza Fm.	Nakrut Fm.	Minkuchar Fm.	Yarmachi Fm.	Bifurak Fm.			
								Yangkazgan Fm.	Karatash Fm.	Atkamar Fm.	Daraitut Fm.	Berkutly Fm.			
								Shuruk Fm.	Kichkinacharvaksay Fm.			Archali Fm.			
	Cambrian	Upper			Lyupek Fm.			Tayman Fm.	Kair Fm.			Lolabulak Fm.			
												Chashmakalon Fm.			
											Obikandyn Fm.				
											Aknulla Fm.				
Paleozoic	Ordovician	Middle		Koksay Fm.			Murun Fm.	Djaltrar Fm.			Alhyaul Fm.				
				Djilbirbay Fm.			Djeroy Fm.	Djadyr Fm.			Shahriomon Fm.				
				Telibay Fm.			Roxat Fm.	Aktoyak Fm.			Almalyn Fm.				
								Bokteken Fm.	Ayakumar Fm.						
	Cambrian	Lower										Obizarang Fm.			
Cambrian	Furongian														
Cambrian	Miaolingian														
Cambrian	Series 2														
Cambrian	Terreneuvian														

marine      coastal-marine      terrestrial

**Table 1.** The list of the Paleozoic Formations of Uzbekistan. The Cambrian, Ordovician and Silurian. References: Akhmedjanov *et al.*, 1967, Kurenkov 1983, Mukhin *et al.*, 1989, Zonenshain *et al.*, 1990, Mirkamalov *et al.*, 1991a, 1991b, 1991c, Z. M. Abduazimova 2011, Mikhaylov 2016.

Paleozoic		Paleozoic Formations of Uzbekistan										
Era	Period	South Tien Shan										
		Ustyurt and Central Kyzylkum		Zhetysay		Zarafshan-Turkestan		Middle Tien Shan				
Epoch	Age	Sultanovs	Bukantau	Tamdytau	Kudjuktau	Nuratau	Gissar Range	Zirabulak-Zhetdin	Alai Range	Charantal Range	Kuramin Range	
		Permian	Lopingian									
Wuchiapingian												
Capitanian												
Wordian												
Roadian												
Kungurlian												
Artinskian												
Cisuralian	Sakmarian											
	Asselian											
	Ghazelian											
	Kasimovian											
Carboniferous	Upper											
Carboniferous	Middle											
Carboniferous	Lower											
Devonian	Upper											
	Devonian	Middle										
		Devonian	Lower									

marine [blue box] [orange box] coastal-marine [green box] [red box] terrestrial [orange box] volcanic [red box]

**Table 2.** The list of the Paleozoic Formations of Uzbekistan (continued). The Devonian, Carboniferous and Permian.

References: Akhmedjanov *et al.*, 1967, Kurenkov 1983, Mukhin *et al.*, 1989, Zonenshain *et al.*, 1990, Mirkamalov *et al.*, 1991a, 1991b, 1991c, Z. M. Abduazimova 2011, Mikhaylov 2016

### *1.2.3 Mesozoic rocks*

The Mesozoic deposits within Uzbekistan are represented by all three systems of the Triassic, Jurassic and Cretaceous. In the case of the Triassic, only the Upper Triassic has been recognized. The undivided upper Triassic and Jurassic strata are represented in Chatkal-Kurama ridges and the Fergana region. The Jurassic deposits within Uzbekistan are relatively few. The most significant areas of their distribution are in the southwestern foothills of the Gissar Range and on its southern slopes. It is represented by sedimentary rocks of continental and marine origin. The Cretaceous rocks are widespread in the Uzbekistan and will be thoroughly explained in the next section as it is the main focus of this chapter.

#### *1.2.4 Cenozoic rocks and sediments*

The Cenozoic deposits are most common in almost all parts of Uzbekistan (Figure 2). They occupy all plains, intermountain and river valleys. The Cenozoic period played most important role in the most geological aspects of Uzbekistan. One of them is the incursion of the proto-Paratethys Ocean during the Eocene and this will be introduced in the Chapter II.

Quaternary deposits occupy large part of Uzbekistan, and they are divided into two main groups: marine and continental facies. The marine facies are very limited. The continental facies of the Quaternary in Uzbekistan are very widely developed, have a variety of composition. Their formative process is due to the history of the geological development of Uzbekistan in the Quaternary, during which there was a further growth (after the Neogene) of mountain systems in the central and eastern parts and the associated expansion of river systems both in mountainous regions and plains.

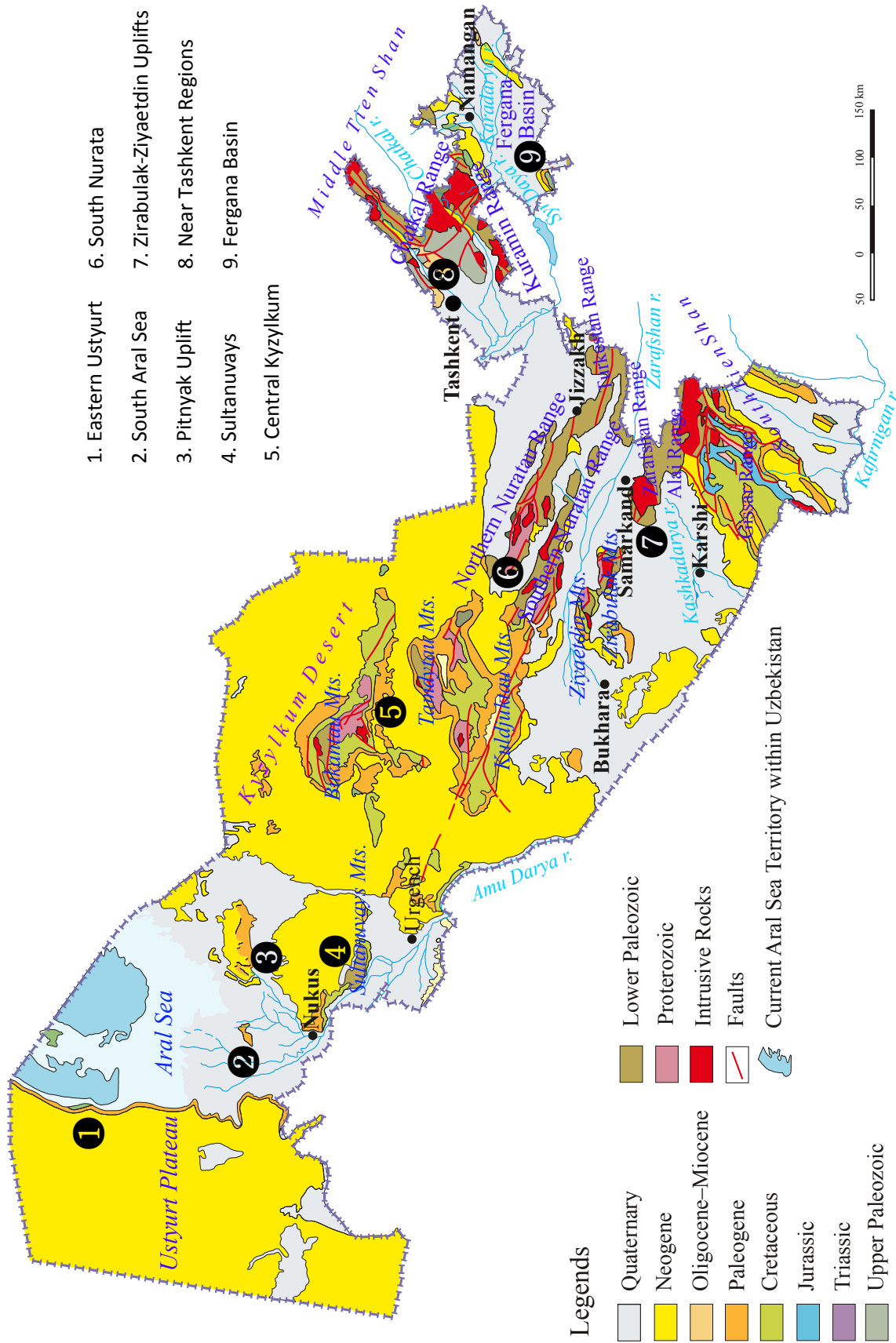
### 1.3. The Cretaceous System of Uzbekistan

The geological research on the Cretaceous deposits of Uzbekistan and Central Asia has a long history and the first time established by Mishenkov (1871), Mushketov (1879, 1886), Romanovskiy (1878-1890), Obruchev (1872) and Berg (1900–1902, 1906).

The first geological expeditions, which started in 1909, conducted a detailed study of the deposits and established a framework of the Cretaceous stratigraphy. The first schemes of the Cretaceous stratigraphy introduced by Mixailkovskiy (1912) for the Central Bukhara, Chernishev *et al.* (1910) for the Fergana Basin, Arkhangelskiy (1916) for Amu-Darya, Ivanov for the near Tashkent regions, Nikolaev, Mashkovtsev and Butov (1924–1927) for the mountain regions of Zeravshan.

The Cretaceous deposits are widely exposed in Western and East Uzbekistan. They are revealed by numerous research methods such as structural geology, drilling methods, and by biostratigraphy of foraminifers, bivalves, cephalopods, gastropods, ostracods, sea urchins, crinoids, vertebrates, plant residues, spores, and pollen. They are characterized by specific lithofacies, and rock associations based on which are distinguished by these rocks and nine regions were allocated: East Ustyurt (No.:1 of Figure 3), South Aral Sea (No.:2 of Figure 3), Pitnyak uplift (No.:3 of Figure 3), the foothills of the Sultanuvais (No.:4 of Figure 3), Central Kyzylkum (No.:5 of Figure 3), South Nurata (No.:6 of Figure 3), Ziyabulak-Zayatdin Uplifts (No.:7 of Figure 3), the near Tashkent Regions (No.:8 of Figure 3) and Fergana Basin (No.:9 of Figure 3) with typical sections distinguished from each other according to the faunistic, lithological and facial aspects (Figure 3. and Table 3.).

The most complete marine deposits of the Cretaceous are distributed in the west of Uzbekistan, lessen in the central part, and intercalated marine and continental facies are mainly distributed in the east of Uzbekistan (Table 3).



1. Eastern Ustyurt
2. South Aral Sea
3. Pitnyak Uplift
4. Sultanuvsay
5. Central Kyzylkum
6. South Nurata
7. Zirabulak-Ziyaetdin Uplifts
8. Near Tashkent Regions
9. Fergana Basin

**Figure 3.** Distribution of the Cretaceous Deposits in the republic of Uzbekistan. Modified after R. X. Mirkamalov (2016) Atlas of Rep. of Uz.



Period Epoch	Regional Correlations of the Cretaceous Formations of the Republic of Uzbekistan																	
	① Eastern Ustyurt	② Southern Aral Sea	③ Pithyak Uplift		④ Sultanways		⑤ Central Kyzylkum			⑥ Southern Nurata	⑦ Zhabulak-Ziaedin Uplifts		⑧ Near Tashkent		⑨ Fergana Basin			
			Western	Southern	Eastern	Bukantau	Dzharakuduk	Kuldjuktou-Auminzatau	Nurata	Tashkent Depression	Near Tashkent Deserts	South and West Shorou, Kyzylbel	South-eastern	Northern				
Cretaceous	Maastrichtian																	
	Campanian	Eastern Ustyurt Fm.																
		Santonian																
	Coniacian	Miyinak Fm.																
		Turonian	Shahaman Fm.															
	Cenomanian	Kenos Fm.																
		Alban	Alkapchigay Fm.															
	Aptian	Sultonbobobo Fm.																
		Barremian	Chimbay Fm.															
	Hauterivian	Valanginian	Aybugir Fm.															
Berriasi		Shakhpakhta Fm.																



**Table 3.** List of the Cretaceous Formations of Uzbekistan.

References: Abduazimova I. M. (1984, 1987, 1988, 2001, 2007, 2011), Arkhangel'skiy A. D. (1916); Alferov G. Yu. (1958, 1969); Jarnyilskaya G. I. (1965); Keshishyan K. A. (1995); Martinson G. G. (1965); Poyarkova Z. N. (1969, 1976); Simakov S. N. (1953); Troitskiy V. I. (2007).

#### *1.4. The aims and purpose of the study*

As the most studies up to now were conducted in Russian the main aim of this chapter was to introduce the general geological outlines of the Uzbekistan and above-mentioned areas by translating them from Russian and comparing with the new research conducted in English.

The attempts on geological correlations of the Cretaceous sequences between the Dzharakuduk Site and Fergana Basin were never done because of the difficulty and especially not well-established stratigraphy and age determinations in the southern Fergana Basin. As described above the Dzharakuduk Site is unique with its richness of the fauna and is much easier to describe the ages by dividing into biohorizons (e.g., Nesov 1978, Veber 1986). On the other hand, the Fergana Basin within the territories of Uzbekistan is not studied very well, as the most studies concentrated only with resource interest. But there were several dinosaurs' findings from the outer part of Uzbekistan, i.e., Kyrgyzstan, Kazakhstan and Tajikistan, which are northern, southern and eastern edges of the Fergana Basin, respectively.

Hereinafter, this research will be the first attempt on the geological correlation between two localities, with the purpose further explorations of the dinosaurs and other fauna of the Cretaceous in the Fergana Basin with the hints of Dzharakuduk.

With this attempt, the northern part of the Fergana Basin, near the Chust City, Namangan Region, Eastern Uzbekistan was chosen, and measurements were carried out in two localities, Gava and Varzyk Provinces, which were described in the Figures 6 to 9.

## **2. The Cretaceous of the Fergana Basin and Dzharakuduk Site: Lithostratigraphy and Vertebrate Fossils**

### *2.1. The Cretaceous Sequences in the Fergana Basin*

The Fergana Basin is one of the largest intermountain depressions of the southwestern Tien Shan, located between the Kuramin and Chatkal from the northwest to northeast, the Gissar, Turkestan and Alai ranges from the southwest to southeast, in the east it is separated from the Central Tien-Shan by the Fergana Range (Figure 4A). The edges of the basin within the borders of Uzbekistan represented by pre-Mesozoic basement rocks, followed by the Mesozoic, the Cenozoic and the central part is covered by the Quaternary sediments (Figure 4B). The basin started to form along the Tien-Shan orogenic belt during the collision of the Kazakhstan micro-continent and the Tarim block in the Late Ordovician (Allen *et al.*, 1992, Cobbold *et al.*, 1996). Repeatedly invasions of the Paleo Paratethys Ocean from west and Paleo-Tethys Ocean from the east during the Mesozoic and Cenozoic resulted in the deposition of the marine sediments (Jolivet *et al.* 2015). The weakening of the crust and the activity of the Talas-Fergana strike-slip fault because of the tectonic collision of the Eurasian and Indian plates, started the shaping the basin. As a result, the basin got its triangle shape, which was remarkably affected by the Talas-Fergana Fault reactivation after by the collision of the Indian plate with Eurasian plate during the Cenozoic (Bande *et al.*, 2015).

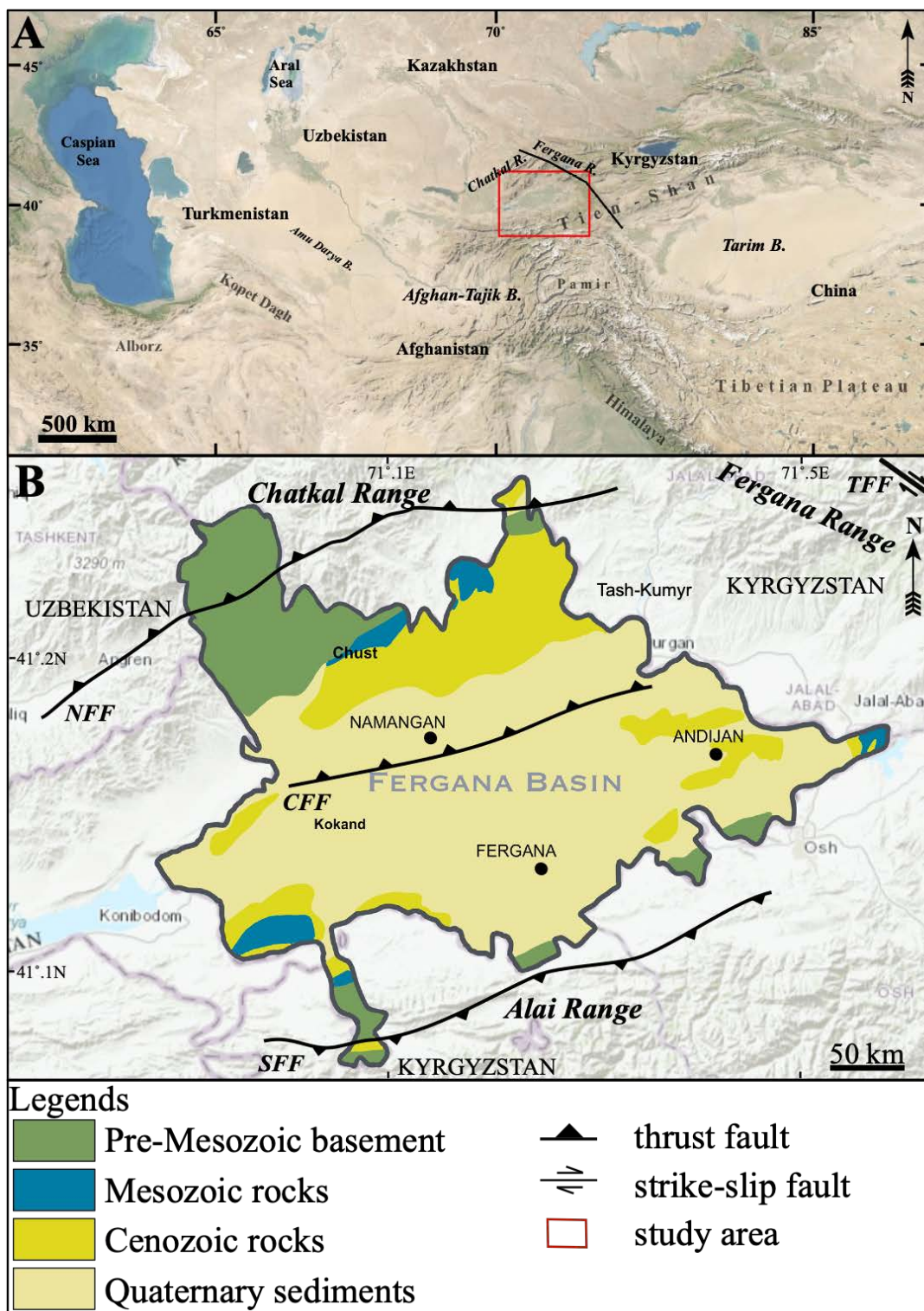


**Figure 4.** Location (A) and Geological (B) Maps of the Fergana Basin. Anvarov *et al.* (2022)

The stratigraphic studies on the Cretaceous system of the Fergana Basin were started at the end of the 19th century by Mushketov (1886, 1906, 1911–1913, 1928), Romanovsky (1878, 1882, 1884, 1890), and continued in the 20th century by Arkhangelsky (1916, 1934), Nalivkin (1926, 1962), Vialov (1936, 1944, 1945), and others. The faunal findings and lithological descriptions of these researchers have provided various local stratigraphic schemes for the Cretaceous deposits mainly distributed in northern and southern, Fergana Basin. The studies of Simakov (1953, 1957), who summarized all the available paleontological and lithological material of the Cretaceous period of Fergana Basin and proposed seven stratigraphic charts. Those studies became of great importance for the development of the stratigraphy of the basin and still in use.




Vialov (1936, 1944, 1945), Verzilin (1962, 1963) and Glumakov (1988) mainly on the south of the Fergana Basin focused on natural resources. But there were still problems on the geochronological point of view. Especially, the Mesozoic deposits of northern part were not differentiated properly. Vialov (1945) and Verzilin (1962, 1963) suggested the existence of the Triassic and Jurassic sediments at the base of northern part of the basin, and according to Vialov (1945) the boundary between the Cretaceous and Paleogene was located at the Coniacian where 400m thick pink loosely cemented sandstones and pebbly conglomerates, dolomites, limestones and scattered calcareous muddy sandstones were interbedded. Verzilin (1962) suggested the boundary at the Lyakan and Sharihan formations (late Albian) and according to the report on oil and gas research by Glumakov (1988) were at the Yalovach and Nichkesay formations (Santonian).

The Cretaceous sequence of the northern margin of the Fergana Basin has been subdivided into the Khodjiabad Fm. (Neocomian–Aptian), Khodjaosman Fm., Alamyshik

Fm. (Albian), Shahrihan Fm., Karaalma Fm. (Cenomanian), Urumbash Fm. (Lower Turonian), Yalovach Fm. (Upper Turonian–Senonian) and Nichkesay Fm. (Campanian–Maastrichtian) (Table 4.). Poyarkova (1976) based on numerous collections of mollusks, mainly marine bivalve established the fossil age of the Cretaceous sequence.

The most recent studies by Abduazimova *et al.* (2011) proposed three stratigraphic schemes: Southern and Western (Shorsu, Kyzylbel), Southeastern (Kuvasay, Muyan and Andijan Uplifts) and Northern provinces (near Chust city, Varzyk provinces) (Table 4). The Northern part of the Fergana Basin characterized by coarse-grained sediments, red in color, where fossils were poorly preserved. The successions combined in the West and South-Eastern part of the Fergana Basin consist of more fine-grained sediments and relatively thicker beds are distinguished, and the preserve of the fossil content were much richer than those of the northern part of the basin. Additionally, the lower Cretaceous (Berriasian-Barremian, Aptian and Albian) sequence located in the Andijan uplifts, South-Eastern Fergana, whereas the Upper Cretaceous has been recognized. According to Abduazimova *et al.* (2011), the base of the Lower Cretaceous in the northern part of the Fergana Basin is composed of the Lower Aptian deposits (e.g., the Khodjaosman Fm.). The Berriasian-Barremian deposits (Khodjiabad Fm.) were observed in the wells of the Andijan uplifts, which were exposed outside of Uzbekistan and represented by pebble conglomerates and coarse-grained reddish-brown sandstones up to 200 meters in thickness.

		IGS	Fergana Basin				
Period	Epoch	Age	Southern and Western	South-eastern		Northern	
			Shorsu, Kyzylbel	Kuvasay, Muyan	Andijan Uplifts		
Cretaceous	Late	Maastrichtian			Nichkesay Fm.	Nichkesay Fm.	
		Campanian	Palvantash Fm.				Yalovach Fm.
		Santonian					
		Coniacian	Yalovach Fm.			Yalovach Fm.	
		Turonian	Oyster Thickness			Urumbash Fm.	
		Cenomanian	Kalachin Fm.	Karaalma Fm.		Karaalma Fm.	
			Kyzylpilal Fm.	Sharihan Fm.		Sharihan Fm.	
	Early	Albian	Lyakan Fm.	Sharihan Fm.		Sharihan Fm.	
		Aptian	Muyan Fm.	Alamyshik Fm.		Alamyshik Fm.	
		Barrem.		Khodjaosman Fm.		Khodjaosman Fm.	
		Hautervian	Khojiabad Fm.				
		Valanginian					
		Berriasian					

 marine
  coastal-marine
  terrestrial

**Table 4.** The list of the Cretaceous Formations of the Fergana Basin. Modified after Abduazimova *et al.* (2011)

At Southwestern Fergana Basin, the Cretaceous sequences were recognized within the foothills of the Guzan Uplift along the Shorsu River (e.g., Abduazimova *et al.* 2011). The Cretaceous rocks along the Shorsu River consist of clastic and carbonate sequence. The lithofacies and yielded fossils have significant differences from Cretaceous formations of Northern Fergana Basin, and the Muyan, Lykan, Kyzylpilal, Kalachin formations, Oyster Thickness, Yalovach, Palvantash and Sariktog formations (Figure 4) were described.



## *2.2 Description of the observed sections in Gava and Varzyk area, northern Fergana Basin*

As mentioned above the most studies were carried out in the western, southern and eastern parts of the Fergana Basin. The northern part has been studied poorly and the lithology for the successions has not studied yet. Therefore, the northern part of the Fergana Basin was selected as the study area, and new data set are provided in this study.

The study area is located at the Northern part of the Fergana basin at the Southern foothills of the Chatkal Range near the Chust city and covers the about 10km area from Southwest to Northeast. Four sections were chosen near the Gava and Varzyk Provinces (Figure 5).

The Cretaceous deposits are very well exposed throughout all the studied sections and are characterized by dark red to brown conglomerates at the base, brick red shales, yellow to gray sandstones in the middle, and oyster shell bed and greenish to yellow shales at the top, with interbeds of caliche abundant paleosols between each sedimentary bed. Trough cross laminations and parallel laminations were observed in conglomerates and sandstones, and these sedimentary structures showing that the sequences are mostly alluvial and fluvial depositions (Figures 6-9).

The Gava and Varzyk sections consist of the interbeds of the clast and matrix supported, pebble to cobble, angular to well-rounded dark red to brown conglomerates with trough-type cross bedding in the base. Followed by the interbeds of the middle to very coarse yellow sandstones, above mentioned conglomerates, red beds of caliche abundant paleosols and fine red mudstones in the middle. The tops of the sections were represented by the interbeds of bivalve abundant, well cemented coarse to very coarse sandstones. The bivalve fossils were recognized as *Pycnodonte* sp., *Liostrea* sp., *Pseudohyria* sp., and *Modiolus* sp. (Figure 11 in Chapter II).

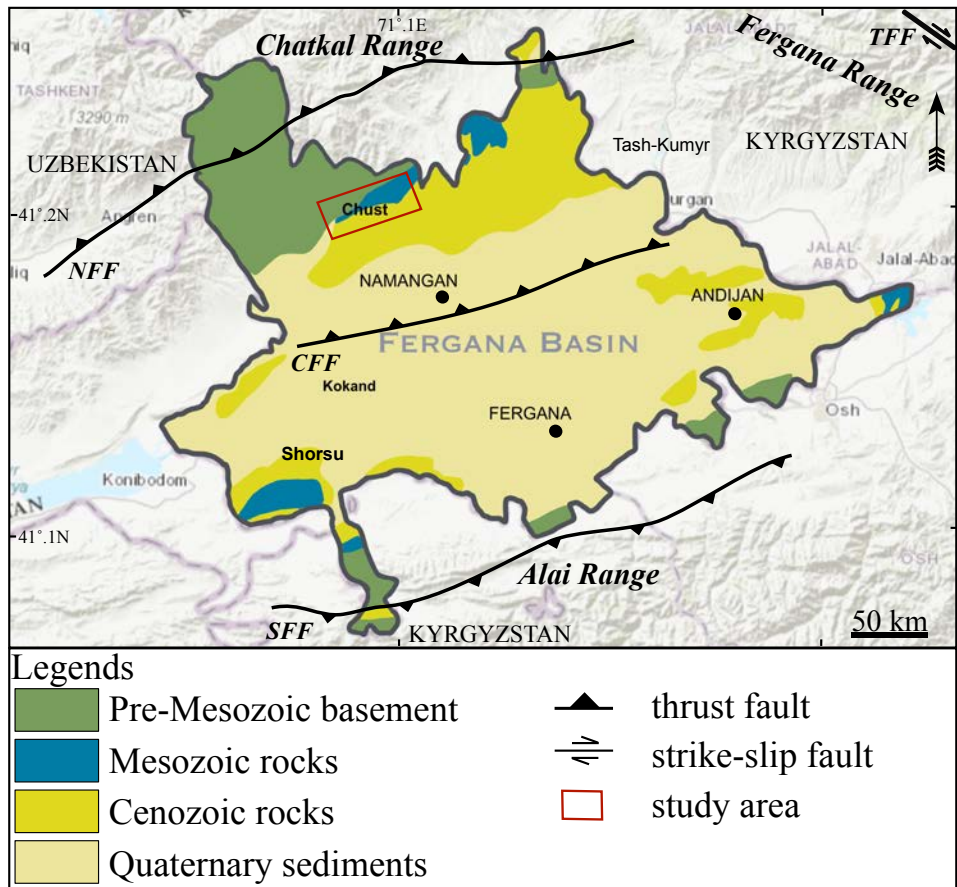


**Figure 5.** Location of the studied area, Northern part of the Fergana Basin. Anvarov *et al.* (2022)

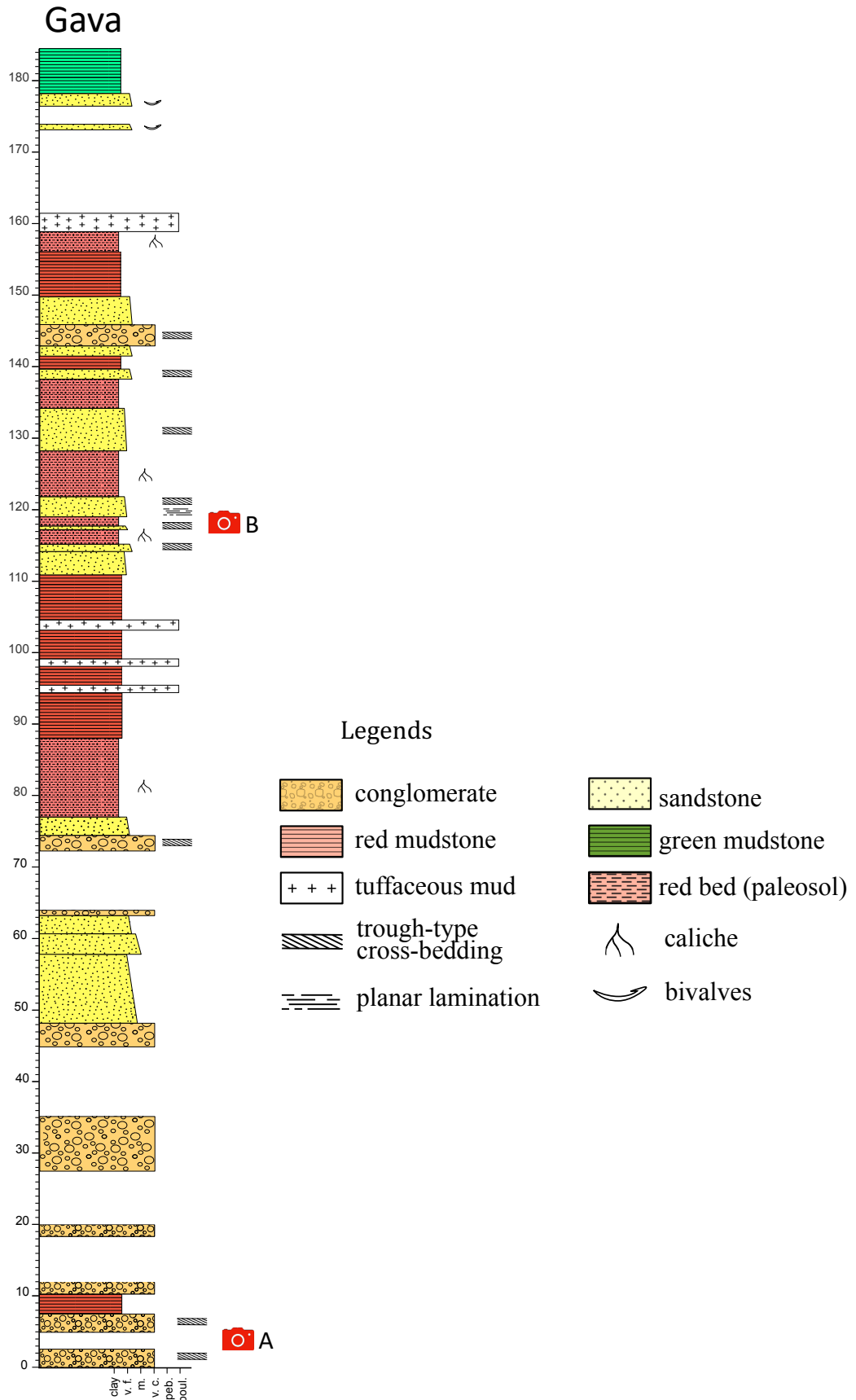


**Figure 6.** Columnar cross-sections of this study Gava Section, photo marks see the next figure.



**Figure 7.** Representative photographs from Gava Section. (A) Trough cross-stratified conglomerate and (B) parallel laminated and trough cross-stratified sandstone.

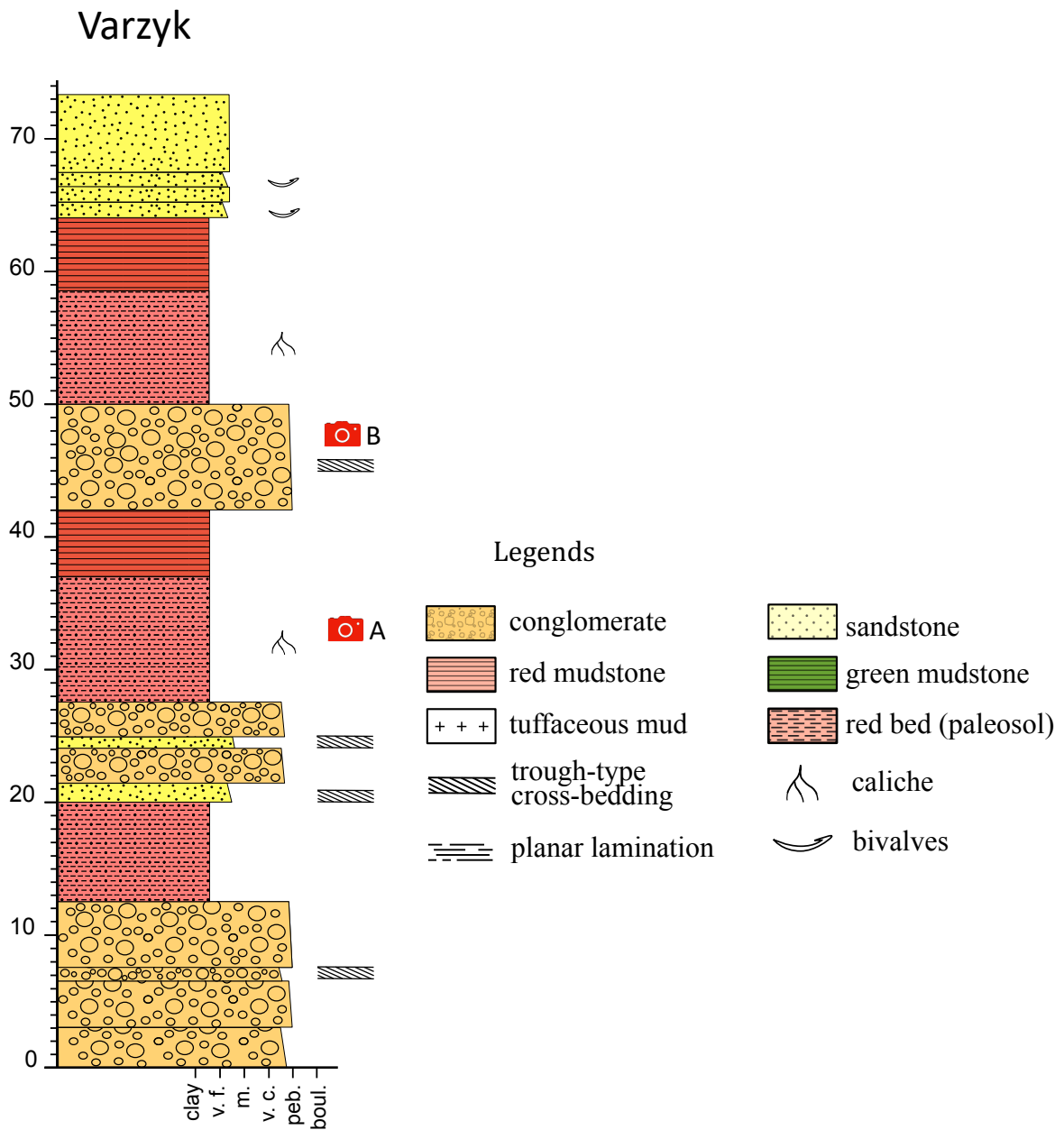


**Figure 8.** Columnar cross-sections of this study Varzyk Section, photo marks see the next figure.



**Figure 9.** Representative photographs from Varzyk Section. (A) caliche abundant red paleosol and (B) planar and trough cross-stratified conglomerate.

### *2.3 The Cretaceous Sequences and Vertebrates Fossils in Dhzarakuduk Site*

The Dharakuduk Site is located at the central part of the Kyzylkum Desert, Central Uzbekistan (Figures 10 and 11). The first geological expeditions started at end of the 18<sup>th</sup> century by the visit of Arkhangelsky in 1887 with the special expedition to Turkestan (current Central Asia). He found fossil bones of vertebrates and fish. Without the idea of the remarkable finding which is the dinosaur bone among the findings in his hand he back to Russia for investigations. His research showed that the bones are remnants of the dinosaurs which previously thought that they were absent in Central Asia. He revisited the Kyzylkum in 1914 and collected much more remains and published his work in 1916 and 1931 related to the dinosaur findings. This was the first step on the explorations of the Dzharakuduk Site.

Further, several expeditions by scientists such as Riabinin (1931), Sosedko (1937), Efremov (1944) Rozhdestvenskiy (1958) were carried out. But the most important contribution was done by Lev Aleksandrovich Nesov, the paleontologist from Leningrad former USSR, who opened new page in the vertebrate paleontology of not only Dzharakuduk Site but also in Uzbekistan. He discovered numerous new localities of the Mesozoic and Cenozoic vertebrates and represented previously unknown fauna of the Cretaceous Uzbekistan (1971–1995). His remarkable works will be introduced later in this chapter.

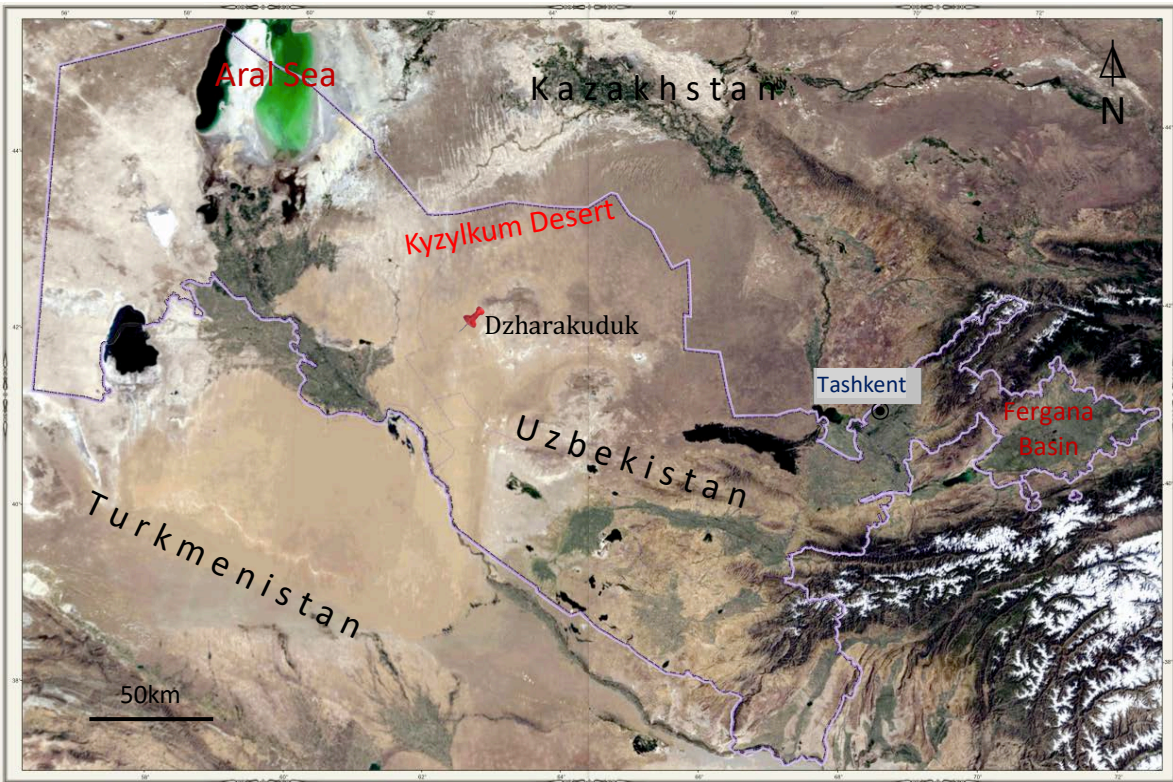


**Figure 10.** The Location map of Kyzylkum Desert and Dzharakuduk Site.





**Figure 11.** The representative photographs of the canyons and cliffs of the Dzharakuduk Site (from URBAC Expedition).




The Cretaceous rocks distributed in the Dzharakuduk Site have been subdivided into the Aptian Kalaata Formation, Albian Djamanyar and Bortesken formations, Cenomanian Urus and Uchkuduk formations, Turonian Djeyrantuy, Kendyktub and Bissekty formations, Coniacian Aytim Formation, Santonian Laulau and Karakatyn formations (Table 5).

The Bissekty and Aytim formations from Turonian and Coniacian are the most important and studied in detail, because of the occurrence of abundant dinosaur specimens.

The Bissekty Formation mainly composed of 80 m thick succession of medium-grained, poorly lithified, cross-bedded fluvial sandstones and clast-supported, well-cemented interbeds of conglomerates, and these deposits have been interpreted as an aggradation 'low-stand' system. The interbedded conglomerates represent flooding surfaces resulting from regional changes in depositional regime following drops in eustatic sea level (Sues *et al.*, 2015; Redman and Leighton 2009).

During the Late Cretaceous times, the region of what is now the Kyzylkum Desert was located at the far western end of the Asian landmass and formed a lowland floodplain setting along the northern margin of Tethys Ocean (Nesov 1995). This coastal plain was habitat to diverse continental ecosystems that prospered under warm, semi-humid climatic conditions. On the other hand, the famous Mongolian and Chinese occurrences, which represent more arid, highland depositional settings, the known fluvial lowland deposits of Uzbekistan did not preserve complete, hinged bones of dinosaurs and other terrestrial vertebrates (Nesov 1995; Redman and Leighton 2009).

IGS			Central Kyzylkum			
Period	Epoch	Age	Bukantau	Dzharakuduk	Kuldjuktau-Auminzatau	
Cretaceous	Late	Maastrichtian	Karakatyn Fm.		Karakatyn Fm.	
		Campanian				
		Santonian	Kynyr Fm.	Laulau Fm.	Kynyr Fm.	
			Aytim Fm.	Aytim Fm.		
		Coniacian	Bissekty Fm.	Bissekty Fm.	Laulau Fm.	
			Turonian	Kendyktub Fm.		
		Cenomanian	Djeyrantuy Fm.			
			Uchkuduk Fm.	Uchkuduk Fm.	Uchkuduk Fm.	
			Urus Fm.	Urus Fm.	Donguztau Fm.	
	Early	Albian	Orazali Fm. & Bortesken Fm.		Uzunkuduk Fm. & Shuruk Fm.	
			Djamanyar Fm.			
		Aptian	Bakhali Fm.	Kalaata Fm.	Kalaata Fm.	
						Tuzkoy Fm. (low)
						Sardoba Fm.
		Barremian				
	Hauterivian					
	Valanginian					
	Berriasian					

 marine
  coastal-marine
  terrestrial

**Table 5.** The list of the Cretaceous Formations of the Kyzylkum Desert and Dzharakuduk Site.

Modified after Arkhangelskiy (1916), Nesov (1978) and Veber (1986).

In total, the remains of representatives of more than 70 vertebrate families were found in the Dzharakuduk Site. It is important that the preservation of most of the residues was excellent. Thus, this fauna has become one of the richest in diversities among those known for the Late Cretaceous, which attracted the specialists from all over the world. Comparison of the Dzharakuduk fauna with other known fauna of the Late Cretaceous showed its similarity, on the one hand, with the fauna of eastern Mongolia and China, and on the other - North America (Nesov 1995; Danilov 2015). The juxtaposition of the Late Cretaceous fauna of Asia and North America, as known currently, is explained by the fact that approximately in the middle of the Cretaceous (Danilov 2015). Such as these parts of the land formed a single continent - Asiamerica, while Europe, on the opposite side, was separated from Asia by the wide Turgai Strait. Modern Central Asia, therefore, was the western outpost of Asia (Nesov 1995; Sues 1995). It was clear that the locations of fossil vertebrates in Kyzylkum were formed in areas of coastal lowlands, like the similar locations of North America. But the conditions were not understood yet as the fact that shark teeth and amphibian bones met together in the Dzharakuduk Site led Nesov to a rather original reconstruction of the conditions of existence of this fauna. The fact is that sharks are typically marine animals, only a few of them can go into fresh waters, and amphibians (frogs, salamanders), at the opposite, habitats of only in fresh waters. In Dzharakuduk, there were teeth of both marine and freshwater sharks. It was logical to assume the existence of such a natural environment that allowed the joint or close existence of both marine and freshwater organisms. Such conditions are created in estuaries - desalinated shallow lagoons and bays of the seas formed at the confluence of rivers into the sea. The change of regimes (marine and freshwater) in this case can be provided by wind surges. Thus, as Nesov thought that there was an alternation of

conditions, favorable either for marine or for freshwater organisms. The remains of vertebrates in Dzharakuduk are confined to the Bissekty Formation, as noted above, dated by Nesov as Turonian–Coniacian, which is the first half of the Late Cretaceous. However, variety of the fossil compositions were similar to those of the North America (Campanian–Maastrichtian), but the same groups of the vertebrates (turtles, dinosaurs, etc.) were much older in the Dzharakuduk Site (Turonian–Coniacian). Therefore, the Bissekty Formation of the Dzharakuduk Site, Central Kyzylkum, is the almost only one place where captures the early Late Cretaceous development of the vertebrates.

Hereinafter, the foreign researchers showed great interest in the fauna of Dzharakuduk. This leads the international expeditions to this location starts from 1994. The Russian leader of the expedition was Nesov, and the American member - a specialist in Mesozoic mammals, professor of the University of California, San Diego, David Archibald. In 1995, Nesov passed away and, the biggest international expedition organized by Archibald named URBAC (after the capital letters of the participating countries Uzbekistan, Russia, Britain, the USA and Canada) began from 1997 in Dzharakuduk. The main aim of the international expedition was to reveal the fauna of the Cretaceous vertebrate of Kyzylkum, including the collection of fossils, clarification of the age of the locations and the conditions of their formation.

The methods of search were consisted of collecting small residues, the most valuable of which are the teeth, jaws and other bones of mammals, using the method of sieving large volumes of rock. Sand from the surface is sifted through sieves with different cell diameters, as a result of which the largest grains of the rock and fossils of a certain size separated. After dry sieving, the remaining rock were washed, dried and sieved again. The concentrate obtained as a result of the described procedure is

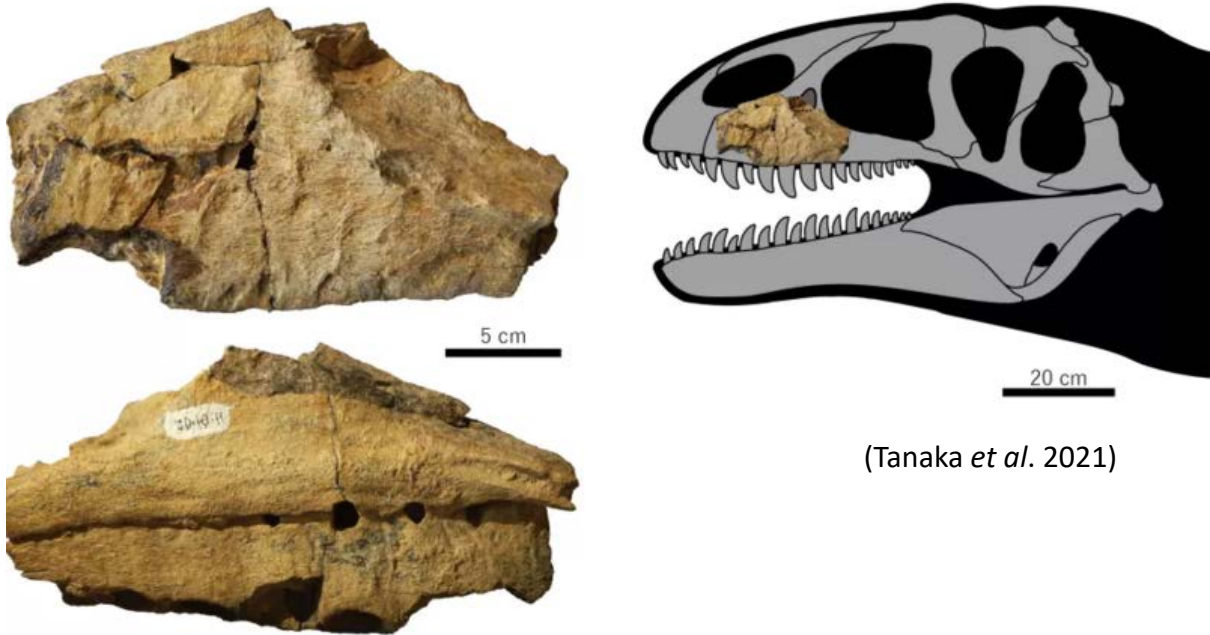
viewed on trays for selecting bone residues. This method allows to process large volumes of rock and not damage fragile fossils. So, only in 2002, 40 tons of rock were checked by the expedition. In addition, the process of selecting materials can be moved to the camp and carried out in more favorable conditions. As a result of the work of the international expedition, the age and geology of the location and composition of the vertebrate complex were clarified. The Bissekty Formation is sandwiched between marine sediments of the middle and upper Turonian (90–92 Ma), and the fauna dates from a narrow interval of 3–5 million years within this interval.

Thus, the fauna of vertebrates has become one of the most accurately dated fauna of the Mesozoic vertebrates for all of Asia. Investigations of teeth of marine sharks in the Dzharakuduk Site reveals that these teeth come from higher horizons of the marine Aytim Formation, and deposits of the Bissekty Formation are alluvial (i.e. terrestrial). The studies of the fossils collected over many years made it possible not only to clarify the composition of the complex, but also to begin a more detailed study of the morphology of individual representatives of this fauna in order to determine their location on the family tree of vertebrates.

Furthermore, the new period begun on the research of not only the Dhzarakuduk but also in Fergana Basin in 2017 between the University of Tsukuba, Japan, State Geological Museum of Tashkent and the State Committee for Geology and Mineral Resources of the Republic of Uzbekistan with the purpose of the geological and paleontological research exchanges. In 2020 the Memorandum of Agreement was signed between two sides on the research exchanges. The first result of this joint program was introduced in 2021, with finding of the new previously unknown species of carcharodontosaurian theropod dinosaur fossil, which were preserved in the State

Geological Museum in Tashkent. The team led by Dr. Kohei Tanaka described this dinosaur as the apex predator of the Turonian ecosystem and named as *Ulugbgsaurus uzbekistanensis* (Figure 12), which means the lizard belonging to Ulugh Bek, who was the most famous scientist and Temurid Sultan from Central Asia, current Samarkand, Uzbekistan during 15<sup>th</sup> century.

A)



(Tanaka *et al.* 2021)

B)



© Julius Csotonyi

**Figure 12.** A) The specimen of the newly discovered carcharodontosaurian theropod dinosaur *Ulugbegsaurus uzbekistanensis* (Tanaka *et al.* 2021), and B) its illustration by Julius Csotonyi.



### 3. Discussions

The measured sections lithofacies and sedimentary structures of the studied sections showed the fluvial environment in the base and the middle, and the top part with fossil assemblage refers to coastal environment for both sections. With this result, it is possible to refer the Yalovach Formation of Abduazimova (2011) only for the base and middle part. The top part, which was described in detail in the next chapter, with high possibility belongs to the Paleogene (Anvarov *et al.*, 2022).

On the other hand, as prescribed above in Dzharakuduk Site, the Bissekty Formation has the similar lithofacies and the bivalve fossils with the same species such as *Modiolus* sp., *Pycnodonte* sp., and *Liostrea* sp., were also found at the upper part of this succession (Figure 13).

Hereinafter, as the result of the first attempt on the correlation of current research is limited only with lithofacies and environmental aspects. But further detailed research must be carried out to fully correlation as the current results from the north Fergana Basin has a great potential on the dinosaur explorations.

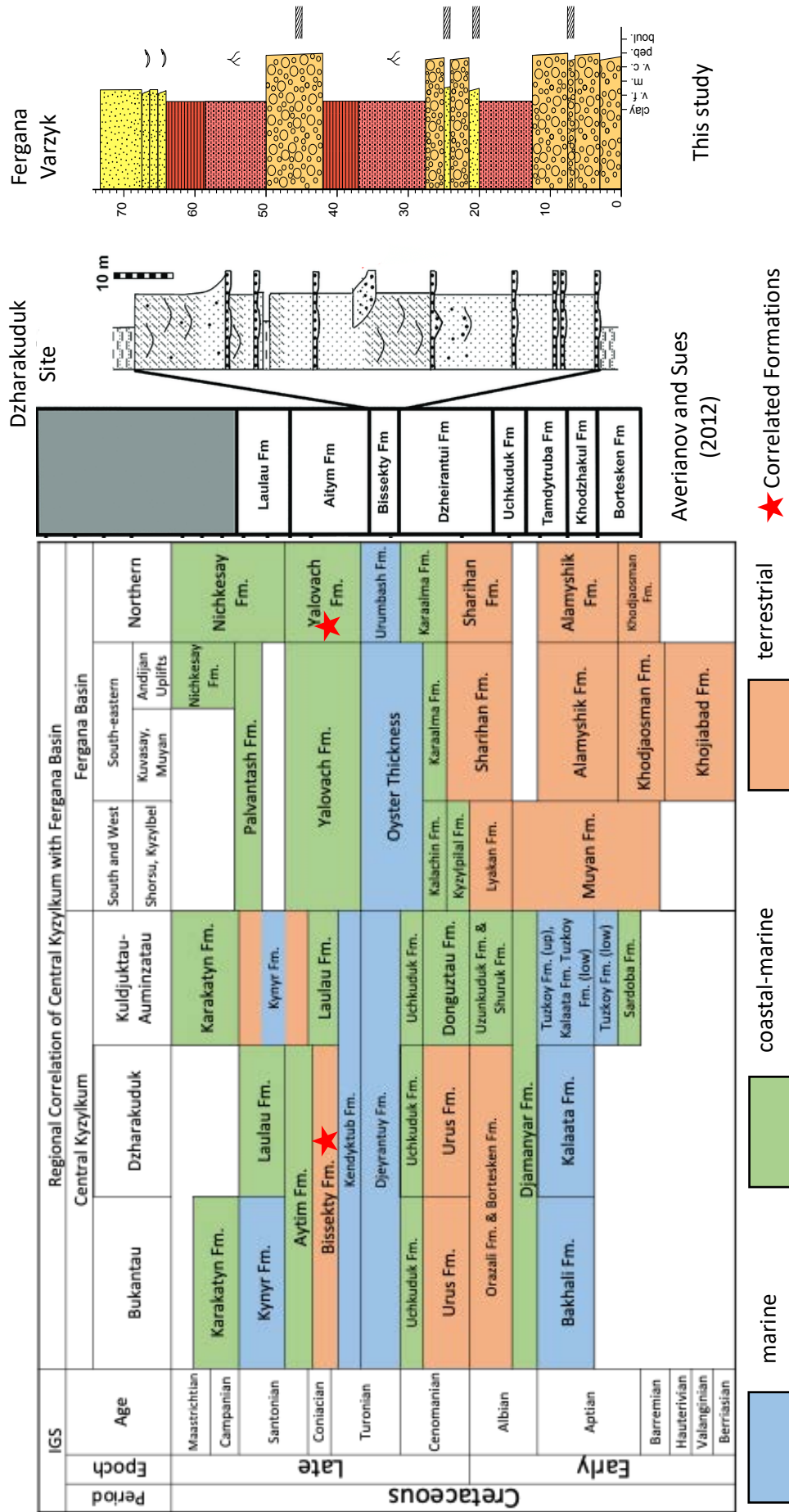


**Figure 13.** The lithological correlations of the Dzharakuduk Site (by Averianov and Sues 2012) and Fergana Basin, Varzyk Section (this study), and their situation in the regional correlation of the Kyzylkum Desert and Fergana Basin.

#### **4. Conclusions**

In this chapter the general geology of Uzbekistan, the Cretaceous of the Dzharakuduk Site Kyzylkum Desert, Central Uzbekistan and the Fergana Basin, Eastern Uzbekistan was reviewed in contrast with the new data obtained from northern part of the Fergana Basin.

The researchers such as Arkhangelskiy and Nesov have a remarkable contribution to the geology of Uzbekistan. With their dedication it is now possible to understand not only the Cretaceous period but also whole paleontology of Uzbekistan.

Now it is relevant to note that some researchers worked on the field of this country brought back all the findings which is legally belong to Uzbekistan and might be the perfect example in the Geological Museum and will be helpful to study and correlate for further research. With the hope for bringing them back and explore more on geology and paleontology of Uzbekistan this chapter reviewed the previous research on the way to introduce to the foreign audience who has an interest on the geology and paleontology of Uzbekistan.

In conclusion, it is relevant to say that the geology of Uzbekistan is unique and important for the revealing and establishing of the geological image of the Central Asia. Especially, the Cretaceous period plays an important role on establishment of the fauna and flora which may fulfil the gaps on the research in paleontology of the Central Asia and the rest of the world.

Among them the Cretaceous Dzharakuduk Site is the most remarkable locality with its exposed sediments of the Cretaceous fauna and Fergana Basin with its potential for further explorations.

Overall, now with this research review, the preliminary image of the geology of Uzbekistan was obtained by translating previous researches from Russian into English and as a result the formations throughout all geological periods were unified. In the

future this will be helpful for the students and researchers who has an interest to geology and paleontology of Uzbekistan.

## **Chapter II: The Fourth Marine Incursion of paleo-Paratethys in the Northern Fergana Basin**

### ***1. Introduction***

The Fergana Basin is among the largest intermountain depressions of the southwest Tien-Shan, located between the northern range of Chatkal and the southern range of Alai. It is separated from the Central Tien-Shan by the Fergana Range in the east (Figures 1A, 1B). The Mesozoic–Cenozoic sediments distributed in the Fergana Basin, along with sediments of the Afghan-Tajik and Tarim basins, have been studied to record the spread of the proto-Paratethys Ocean in Central Asia and the tectonics after collision with the Indian subcontinent. In particular, from the Mesozoic to the early Cenozoic, sedimentary sequences of the three basins indicate the repeated deposition of terrestrial and marine sediments and have been interpreted as recording transgression and regression of the proto-Paratethys Ocean (e.g., Burtman, 2000; Bosboom *et al.*, 2017; Jolivet, 2017).

The Fergana Basin, which is the focus of this study, is surrounded by the Chatkal Range, Alai Range, and Talas-Fergana Fault on the north, south, and east sides, respectively, and has a unique triangular shape (Figure 1B). While there are several studies focusing on the sedimentary rocks of the Afgan-Tajik and Tarim basins and the stratigraphy of the Mesozoic and Cenozoic have been established, stratigraphic studies of the Fergana Basin are insufficient.

Previous studies focusing on the Fergana Basin by Vialov (1936, 1944, 1945), Verzilin (1962, 1963), and Glumakov (1988) were mainly concentrated in the south of the basin, where natural resources are the most important. However, problems from a geochronological point of view remained, and the Mesozoic deposits of the northern part remain undifferentiated. Studies by Vialov (1945) and Verzilin (1962, 1963) suggested the existence of Triassic and Jurassic sediments at the base of the northern part, whereas

the most recent study by Abduazimova *et al.* (2012, 2012) recognized the Lower Cretaceous Aptian-Albian stages and all stages of the Upper Cretaceous in the north of the basin.

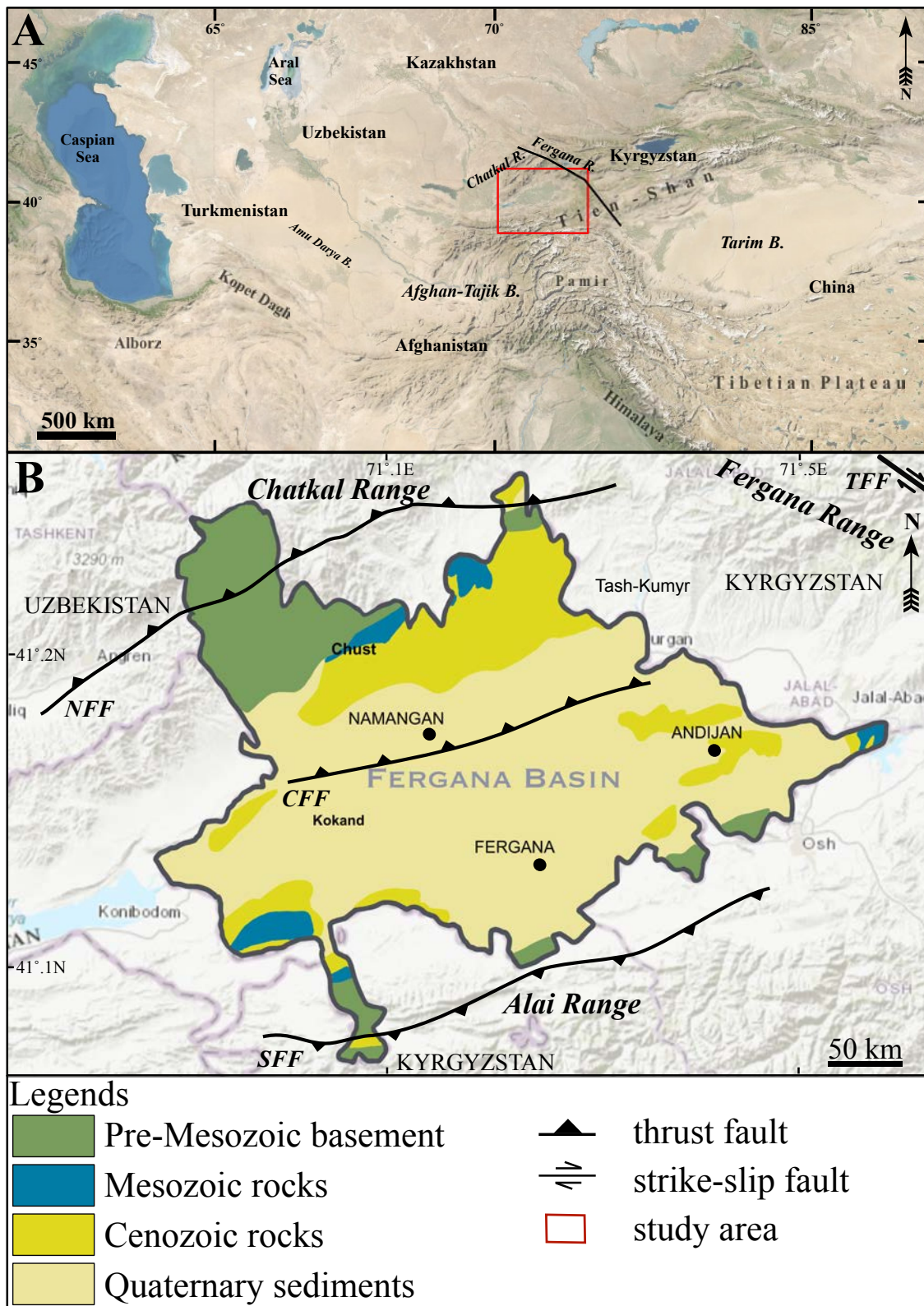


**Figure 1.** A). The index map of Uzbekistan with location of the Fergana Basin and adjacent areas of central Asia. B) The Geological map of the Fergana Basin modified after Mirkamalov (2016). TFF-Talas Fergana Fault; NFF-North Fergana Fault; CFF-Central Fergana Fault; SFF-South Fergana Fault.

The stratigraphy of the basin was studied by the Geological Survey of Uzbekistan during 2007–2012. The age of the sequences was determined by the stratigraphy and yielded fossils such as foraminifers and mollusks, which suggested the existence of all sections of Cretaceous sediments in the northern part of the basin. However, in these studies, no columnar sections or identified fossils were shown (illustrated) in the reports; thus, comparison and verification cannot be sufficiently performed. It is required to fully describe the measured columnar sections and yield fossils to perform the geological correlation with the stratigraphy and ages, and their interpretation of geological events that have recently become evident in the Afghan-Tajik and Tarim Basins. From this perspective, this study investigated and examined the Cretaceous–Paleogene strata in the northern part of the Fergana Basin in 2017 and 2018. The study area is located in the northern part of the Fergana Basin at the southern foothills of the Chatkal Range near Chust City and corresponds to a range of approximately 10 km from southwest to northeast. Four sections were chosen for the study near the Gava and Varzyk provinces and the Karabulak water dam (Figure 2). This study describes the measured columnar sections and report the results of the geological age examined by sulfur and strontium isotope analyses.



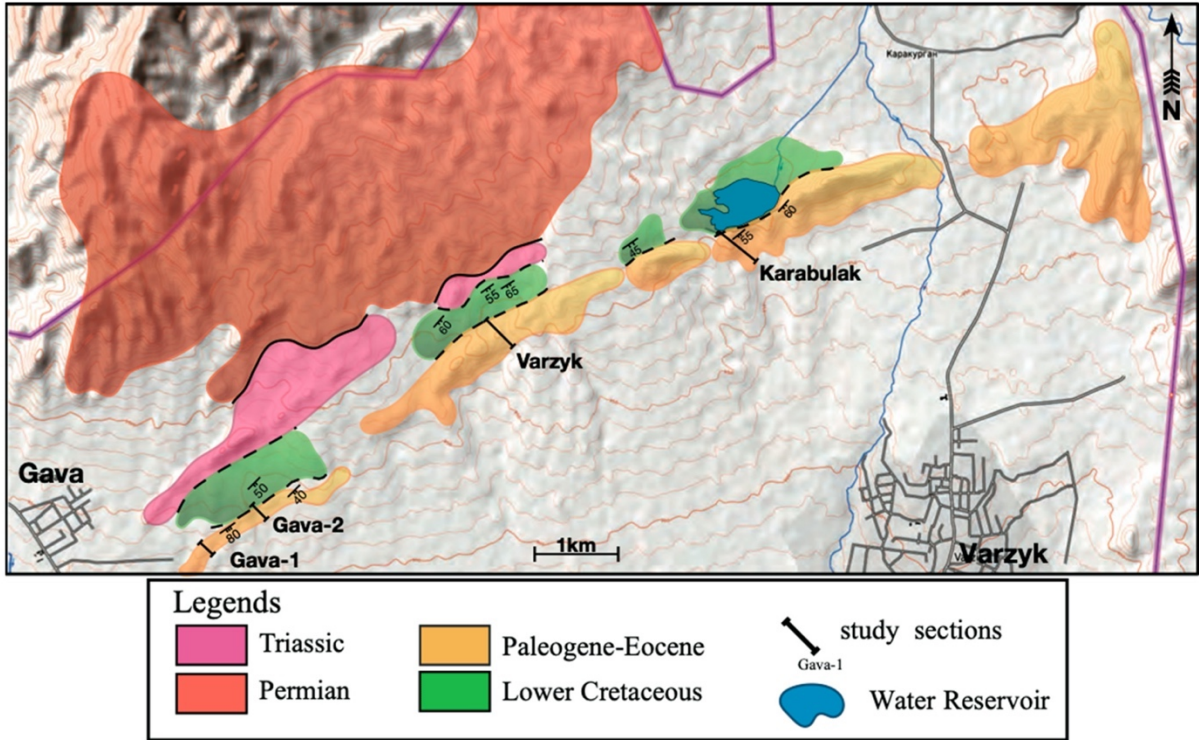


**Figure 2.** The geological map of the northern part of the Fergana Basin within the territory of Uzbekistan with the locations of studied sections near the Gava and Varzyk Provinces and Karabulak water dam.

## **2. Geological Outlines of the Paleogene Northern Fergana Basin**

The Fergana Basin is bounded by thrust faults in the north and south, bordering the Chatkai Range in the north and Alai Range in the south. The northeast side of the basin is bounded by the Talas-Fergana Fault (TFF) of the dextral strike-slip fault (Figures 1A, 1B). These faults were caused by the collision with the Eurasian continent and the Indian subcontinent owing to the northward movement of the latter after the Eocene (Burtman and Molnar, 1993; Burtman *et al.*, 1996). The basin has been proposed to have formed owing to late Paleozoic to early Mesozoic (Permian to Triassic) rifting of the Paleozoic basement, and mainly Permian–Early Triassic volcanic rocks, Jurassic coal facies, and Early Cretaceous continental deposits have filled the depression basin (e.g., Abduazimova *et al.*, 2012, 2012; Pomazkov, 1972; Jolivet, 2017).

In the northern Fergana Basin, the study area is predominantly occupied by Permian igneous rocks, Triassic continental deposits, Cretaceous to Paleogene sedimentary rocks, and Quaternary sediments (Figure. 2). Mesozoic to Quaternary sedimentary rocks and sediments trend approximately north–south and dip to the east. The Permian rocks are represented by granodiorite, alkaline basalt, and gabbro, and the absolute ages of these rocks are  $299 \pm 16$  Ma for granodiorite and  $252 \pm 13$  Ma for alkaline basalt, according to radiometric measurements by Askarov *et al.* (1974). The only continental Lower Triassic is distributed and unconformably overlies Permian igneous rocks, although the Middle and Upper Triassic are missing. Jurassic coal-bearing formations are distributed in the northern Tash-Kumyr region of Kyrgyzstan, with interbeds of sandstone and shale containing the lenses of lacustrine bauxites and bauxite rocks in the south (Nalivkin, 1962; Abduazimova 2012, 2012; Bande *et al.* 2017). The deposition of the coal-bearing facies ended with the development of the Upper Jurassic and Lower Cretaceous red beds. The stratigraphic and sedimentology analyses by Jolivet (2017) from the adjacent areas

of the Fergana Basin, such as the Tash-Kumyr, Kalaza, Tarim, and Junggar areas, suggest that the tectonic activities continued during the Jurassic and Cretaceous transition, and the change between sedimentary facies from sandy to conglomeratic deposits was highly linked with the expansion of the arid climate. At the northern edges of the basin, Jurassic deposits are represented by purple to dark red conglomerates, and Cretaceous deposits containing oyster beds are indicated (Vialov, 1944).

In almost all sections of the basin, the Paleogene deposits were strongly deformed owing to the tectonic activities of the Cenozoic orogeny. The main factor causing deformation, as suggested by Bande *et al.* (2017), is the activity of the Talas-Fergana Fault after the rapid exhumation event at 25 Ma at the northwest Tien-Shan due to the collision of the Indian subcontinent with Eurasia that started at approximately 50 Ma and continues today. The activity of the Talas-Fergana Fault and northward compression of the Pamir Range still reshaped the basin and caused counter-clockwise rotation of the northwestern edges (Figure 1B).

### *2.1. Limestone-clastic sequence in the northwestern Fergana Basin*

A laterally continuous limestone-clastic sequence covering 10 km occurred in northwestern Fergana Basin. The conspicuous sequence is composed of two or three limestones and intercalated fine-grained sandstone and red beds. This sequence can be observed at three localities, Gava, Varzak, and Karabulak, from west to east. The Gava section consists of Gava-1, which is along the village road, and Gava-2, which is approximately 500 m eastward (Figure 2). In this chapter, the Karabulak section corresponding to the type section of the limestone-clastic sequence is described first, followed by the respective section (Figure 3). Each section is treated here as the upper “limestone-clastic sequence” and the lower “underlying sequence” for highlighting the “limestone-clastic sequence.”

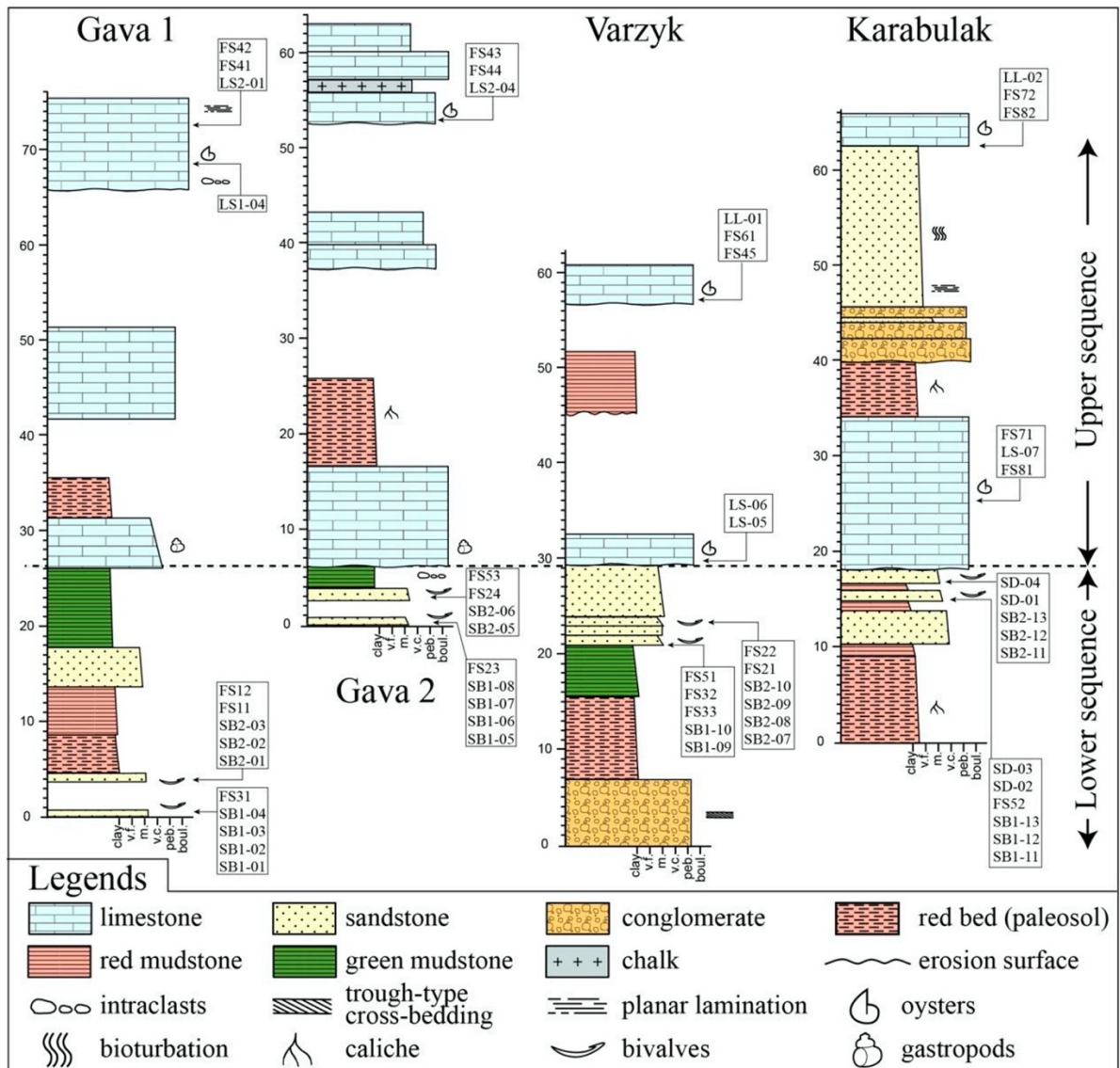


**Figure 3.** The columnar sections of the study area in the northern part of the Fergana Basin within Uzbekistan

### 2.1.1. Karabulak Section

This section is located at the southern bank of the water reservoir and the lower sequence is composed of coarse-grained clastics (Figures 2 and 3). Its thickness is more than 15 m and upper part is comprised of medium- and coarse-grained sandstone accompanied by sandy shell beds (Figure 4D). These sandy shell beds are developed in at least two stratigraphic levels at a 1 m interval. The presence of shell beds is remarkably different from the case of the limestone beds in the upper sequence. Microscopic observations showed that the sandy-shell bed consists of quartz grains within a sparry calcite cement matrix. Plagioclase and calcite grains are also present as minor components, although monocrystalline quartz is predominant. These grains are medium- to coarse-grained, very angular to angular, and poorly sorted (Figures 8C,D). In addition, the lower part of the Karabulak section is comprised of a red bed that is approximately 8 m thick. The red bed contains characteristically reworked calcareous nodules (Figure 4E), which may be of caliche origin. Thus, the red bed has been classified as a paleosol (Surakotra *et al.* 2018).

As shown in Figure 3, the upper sequence is characterized by intercalated limestone beds and begins with 15 m-thick limestone, followed by 30 m-thick mudstone and fine-grained sandstone with conglomeratic beds, and then 5 m-thick limestone, in that order (Figure 5A). The two limestone beds of the upper sequence are rich in oyster shells and represent coquina-shell beds. Microscopic observations show that the lower limestone predominantly consists of several fine-grained fragments of calcareous bioclasts, such as bivalve shells and corals, while the upper limestone is characterized by the presence of microoncooids, oolite grains, and bioclastic fragments (such as gastropods and bivalves) within a dusty matrix (Figure 8G,H). In addition, it should be noted here that the clastics are red in the lower part and yellowish gray in the upper part, and so the transition from

the red bed to the upper limestone can be distinctly observed (Figure 5B). As depicted in Figure 5C, the crudely bedded red bed consists of mudstone in addition to some pebbles and cobbles, and it is overlain by a clast-supported conglomerate (Figure 5D). This conglomerate consists of pebbles and cobbles and is subangular to subrounded clasts composed of fine-grained sandstone approximately 5 m in thickness. This conglomerate is also crudely bedded with fine-grained sandstone and overlain by parallel laminated fine- to very fine-grained sandstone, approximately 3 m thick (Figure 5E).

It should be noted here that the sandstone is characterized by the intercalation of a matrix-supported conglomerate, in which burrows are developed (Figure 5F). More specifically, burrows developed in the 3 m-thick fine-grained sandstone overlying the parallel-laminated sandstone unit. As shown in Figure 5F, the burrow density increases upward, and the burrow-containing sandstone is overlain by shell beds (Figure 4A) ranging from 10 cm to 1 m in thickness (Figure 4B). The accumulation of shells was found to be considerably dense (Figure 4C), and the total thickness of the shell bed was determined to be 5 m.

This sequence of red beds, conglomerates, burrow sandstone, laminated sandstone, and shell beds represents the main facies of the Cenozoic System in the northeastern Fergana Basin, thereby suggesting a transgressive sequence.

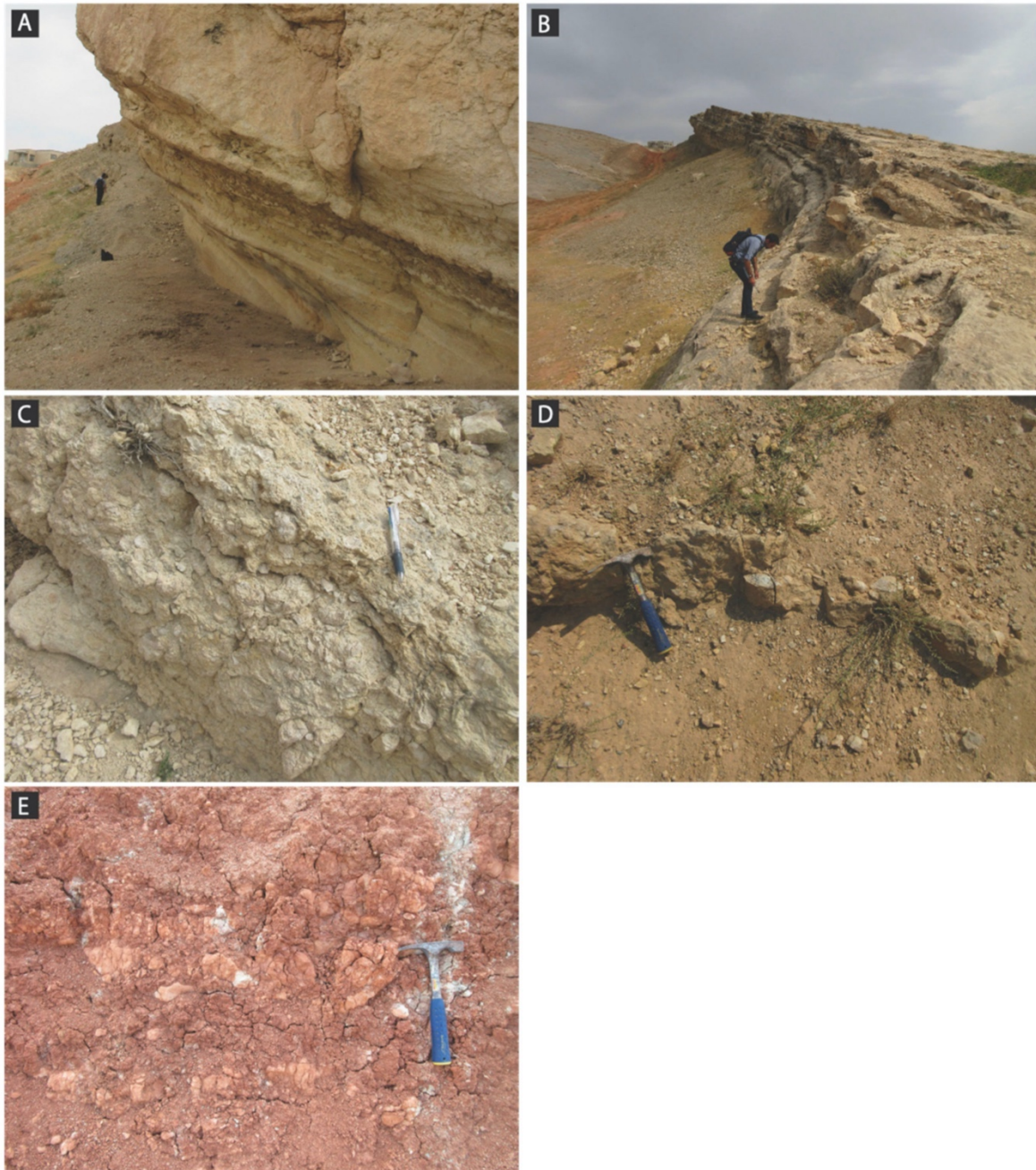


**Figure 4.** The field photographs of the sedimentary rocks at the Karabulak section. (A) Transition of parallel sandstone to burrow-containing sandstone. The density of the burrows increased in the upward direction. (B) Bedded shell beds, which overlie the burrow-containing sandstone. (C) Close-up of the shell beds. (D) A shell bed in the lower sequence. (E) Caliche in the red beds of the lower sequence.



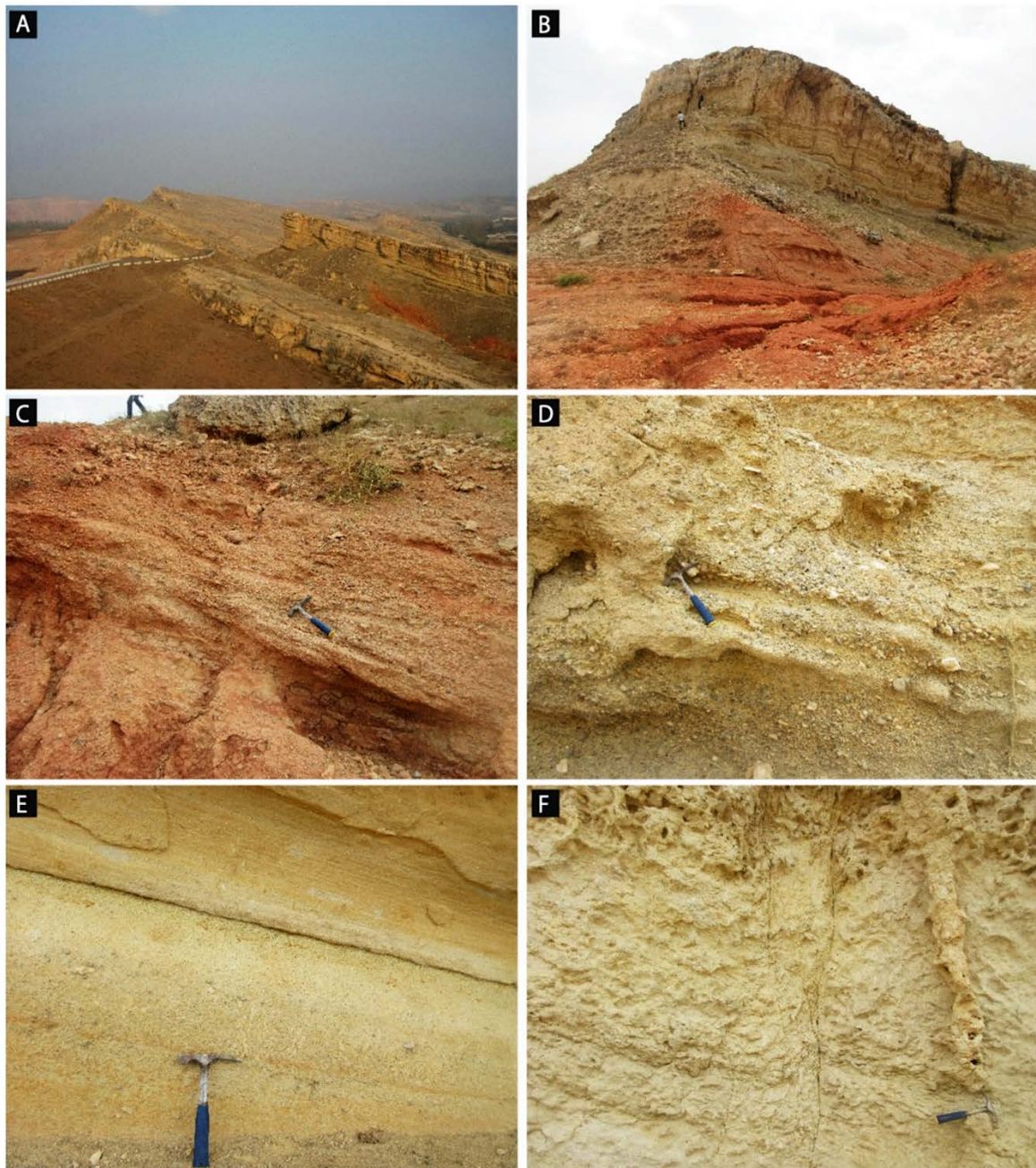


**Figure 5.** The field photographs of the sedimentary rocks at the Karabulak. (A) Eastward view from Karabulak, where two limestone beds and intercalating beds can be observed. The lower left part of the view shows the reservoir dam. (B) Clastics and overlying limestone. The clastics part was comprised of red beds, conglomerates, and fine-grained sandstone. (C) Red beds of conglomerate. Some low-angled cross-beds can be observed. (D) Crudely stratified conglomerate. Some clasts are sub-angular. (E) Parallel laminated fine-grained sandstone. A small number of burrows developed sporadically. (F) Densely developed burrows in the fine- to very fine-grained sandstone.

### *2.1.2. Varzyk Section*

The lower sequence of the Varzyk section is composed of conglomerates, red-green beds, and fine-grained sandstone, in ascending order. As shown in Figure 6D, the total section of the lower sequence, approximately 30 m thick, observed precisely, and the conglomerate consists of rounded pebbles within a muddy matrix. In addition, the conglomerates are crudely stratified, and are overlain by red-green beds composed mainly of mudstone (approximately 15 m thickness), and fine-grained sandstone. The red-green beds are composed mainly of mudstone. The sandstone bed sporadically yields shell fossils (Figure 6E).

Two shell beds of limestone are present in the upper sequence of the Varzyk section, wherein both the lower and upper shell beds create ridges in the cuesta topography (Figure 6A). The red beds between the two shell beds are strongly weathered, and as a result, the relationship between the lower and upper shell beds cannot be observed (Figure 6B). Indeed, the red beds are observed only along the artificially excavated trench (Figure 6C). Furthermore, the lower limestone was approximately 3 m thick, whereas the upper limestone is approximately 4 m thick. The stratigraphic gap between the two limestone beds is estimated to be 25 m at least, and the red beds occupy the upper parts. Both limestone levels are thickly bedded and are a few dozen centimeters thick. The lower beds characteristically yielded abundant oyster shells (Figure 6B).

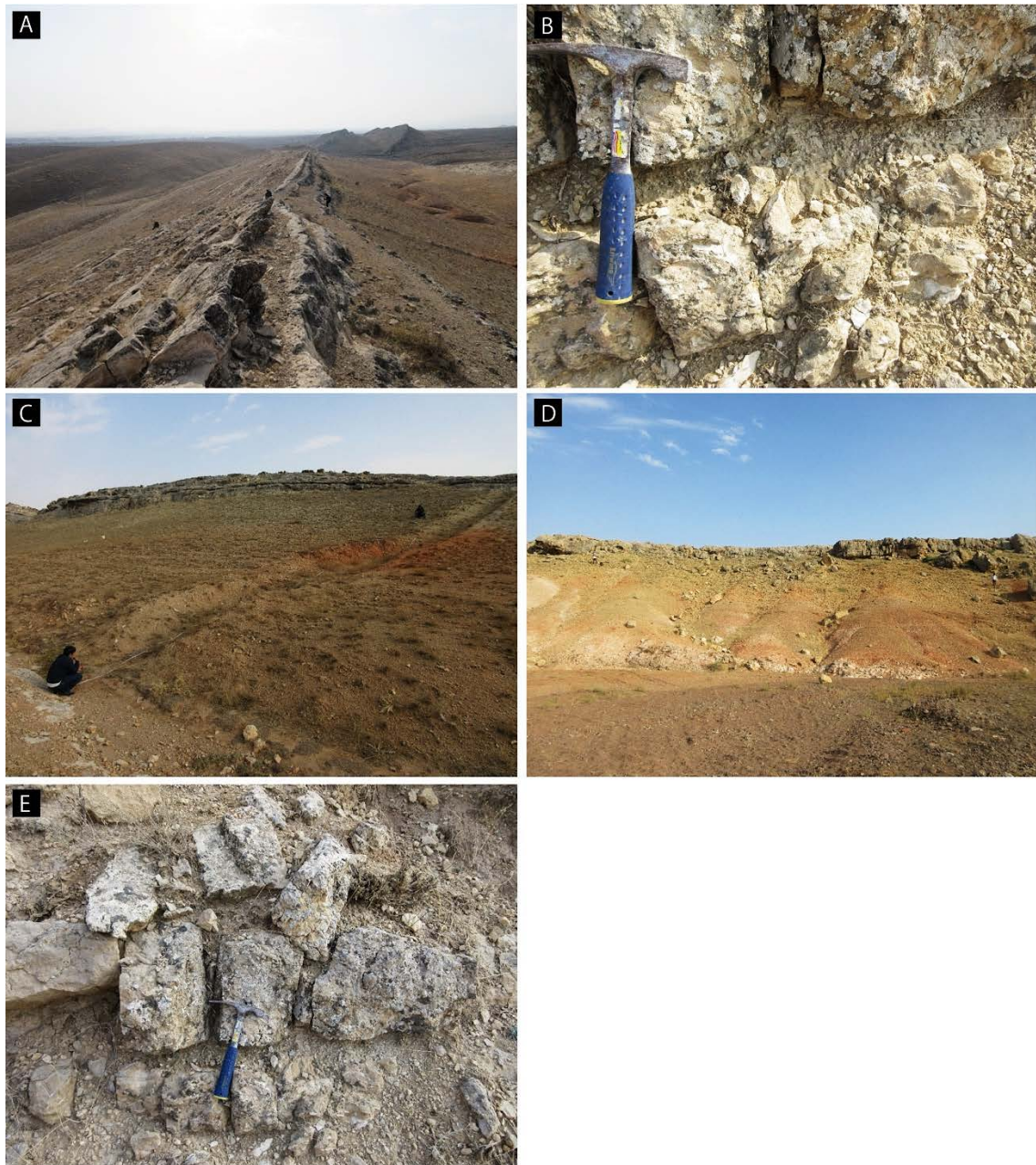


**Figure 6.** Field view of the sedimentary rocks at the Varzyk section of the northern Fergana Basin. A) Westward view at Varzyk. The cuesta topography is composed of limestone beds. B) Close-up view of the lower limestone area, which is composed of oyster shells. C) Red beds and the trench between the two limestone beds. D) The lower sequence and the lower limestone area of the upper sequence. E) Conglomerate of the lower sequence. Note that conglomerate is poorly sorted and clast-supported.

### *2.1.3. Gava – 1 and Gava – 2 Sections*

The Gava section is comprised of both Gava-1 and Gava-2. The lower sequence is moderately well exposed in the Gava section, and in particular, in the Gava-2 section, the shell bed is present approximately 3 m below the upper sequence (Figures 3 and 7B,C). The microscopic features of the shell beds at Gava-1 were comparable to those of the Karabulak section, wherein several very angular quartz grains are present within the sparite matrix containing bivalve shells (Figures 8C,D). The lower sequence is underlain by various colors of mudstone intercalating the shell beds. Mudstone, red-green beds, and conglomerates are also exposed in the lower sequence.

The upper sequence of the Gava section is comprised of three limestone beds (Figures 3 and 7A), unlike in the case of the Karabulak and Varzyk sections. More specifically, the lower two limestone beds intercalate with red beds, although there is no rock exposure in the upper interval between the upper limestone beds. Furthermore, the lower and middle limestone beds can be observed in the Gava-1 section (Figure 7D). In this case, the lower limestone bed is crudely stratified, is rich in oyster shells, and is categorized as a coquina bed (Figure 7E). It is also overlain by a 4 m-thick red bed. The middle limestone bed is micritic, and no fossils have been detected thus far (Figure 7F,G). The middle limestone bed is also thick and crudely stratified. In contrast, the upper limestone layer yields abundant oyster shells, and based on microscopic observations, it has been categorized as an oncoidal and bioclastic grainstone (Figures 8E,F). Several oolitic grains and bioclastic fragments, such as bivalves, gastropods, and foraminifers, are also present within a sparry calcite cement matrix, while the microscopic bio-skeletons and fragments with diameters less than 1 mm have been identified as microlite-coated cortoid particles.

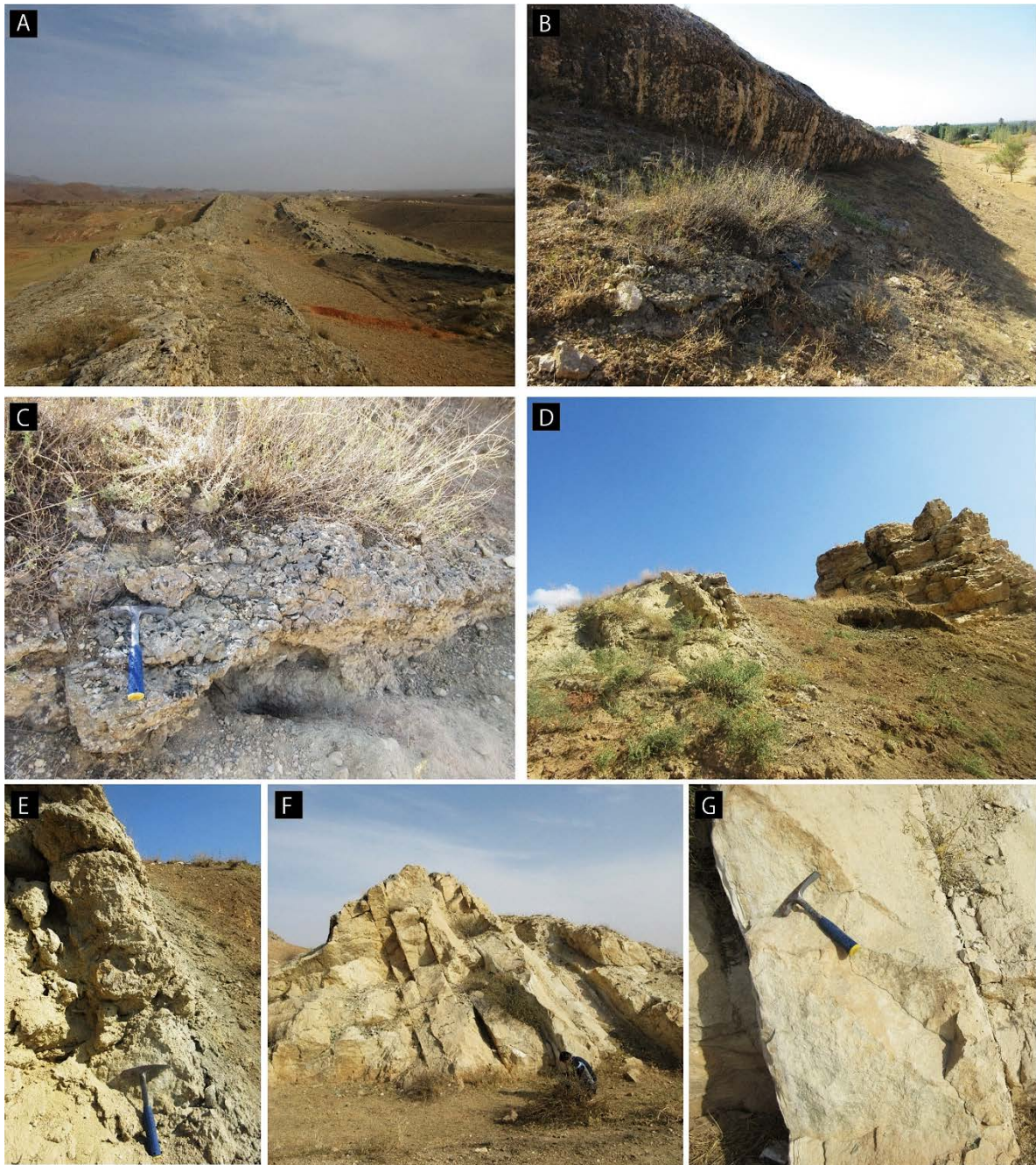


**Figure 7.** The photographs of the sedimentary rocks at the Gava. A) Eastward view at Gava. The upper (third) limestone area can be observed in the middle-right section of the image. B) Lower limestone area of the upper sequence and the shell bed of the lower sequence. C) Close-up image of the shell bed of the lower sequence. D) The lower sequence (left) and the upper sequence (right). E) Close-up image of the boundary between the limestone and the overlying red bed. The outcrop corresponds to that shown in Figs. 3–4. F) The middle limestone bed of the upper sequence. The limestone is crudely stratified. G) A close-up image of the middle limestone area.

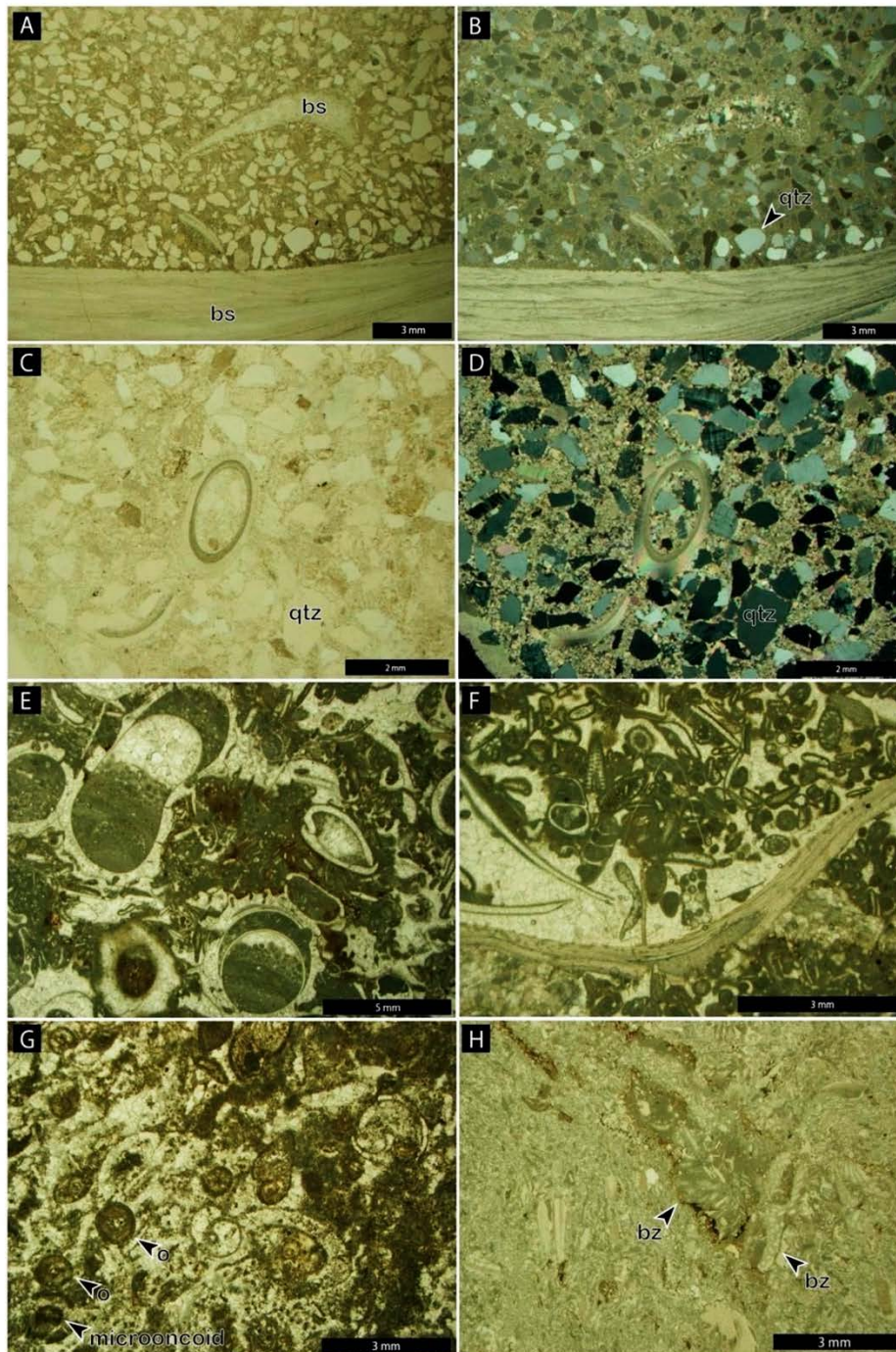


**Figure 8.** Photomicrographs of limestone and clastic sedimentary rocks in the study section. (A,B) Shell bed of the lower sequence of the Gava-1 section (sample number, SB1-02) containing bivalve shells (bs) and very angular medium- to coarse-grained quartz (qtz) grains. (C,D) Shell bed of the lower sequence of Karabulak section (sample number, SB1-12). (E) Bioclastic packstone of the upper sequence of the Gava-1 section (sample number, LS2-01). (F) Oncoids and bioclastic grainstone of the Gava-1 section (sample number, LS1-04). (G) Bioclastic limestone of the upper sequence of Karabulak section with oolite grains (o). (H) Bioclastic limestone of Karabulak section (sample number, LS-07) including fragments of bryozoa (bz).

### **3. Methods**

#### *3.1. Sampling and preparation for isotope measurements*

Investigated bivalve fossil shells and limestone rock samples were collected during two field expeditions in 2017 and 2018, from the Cretaceous and Paleogene successions at four localities. The sections were described bed – by – bed for lithology, texture, size, color, fossil content and sedimentary structures. Altogether seventy-eight (n=78) fossil, sandstone, conglomerate and limestone samples were collected. A seventy (n=70) fossil and limestone samples were selected for stable isotope measurements.

From the samples collected bivalve fossil shells (n=56) and limestone rock samples (n=3) were chosen for the stable isotope analysis. A list of the collected samples is given in Table 1, and the sample collection level for each section is shown in Figure 3.

Section	Sequence	Sample No	Lithology	Material	S <sub>CAS</sub> (wt%)	Error	δ34S	Error	<sup>87</sup> Sr/ <sup>86</sup> Sr	2SE Error				
Gava 1	upper	FS42	Limestone Bed	Oyster	0.141	0.004	19.988	0.745	0.707826	0.000006				
		FS41	Limestone Bed	Oyster	0.220	0.003	20.128	0.066						
		LS2-01	Limestone Bed	Oyster	0.093	0.006	21.193	0.111						
		LS1-04	Limestone Bed	Limestone	0.026	0.001	19.437	0.080						
	lower	FS12	Shell Bed	Bivalve	0.160	0.001	16.627	0.067	0.707772	0.000006				
		FS11	Shell Bed	Bivalve	0.136	0.007	16.429	0.094						
		SB2-03	Shell Bed	Bivalve	0.157	0.004	16.663	0.130						
		SB2-02	Shell Bed	Bivalve	0.212	0.005	16.633	0.096						
		SB2-01	Shell Bed	Bivalve	0.175	0.002	16.638	0.106						
		FS31	Shell Bed	Bivalve	0.271	0.011	14.936	0.055						
		SB1-04	Shell Bed	Bivalve	0.181	0.002	16.523	0.116						
		SB1-03	Shell Bed	Bivalve	0.226	0.007	16.439	0.137						
		SB1-02	Shell Bed	Bivalve	0.218	0.002	16.454	0.087						
		SB1-01	Shell Bed	Bivalve	0.238	0.002	16.445	0.126						
Gava 2	upper	FS43	Limestone Bed	Oyster	0.188	0.002	20.888	0.076	0.707812	0.000005				
		FS44	Limestone Bed	Oyster	0.142	0.006	19.448	0.074						
		LS2-04	Limestone Bed	Oyster	0.047	0.002	19.372	0.096						
	lower	FS53	Shell Bed	Bivalve	0.237	0.003	16.242	0.061	0.707794	0.000007				
		FS24	Shell Bed	Bivalve	0.207	0.003	16.063	0.070						
		SB2-06	Shell Bed	Bivalve	0.193	0.001	16.378	0.090						
		SB2-05	Shell Bed	Bivalve	0.172	0.001	16.759	0.078						
		FS23	Shell Bed	Bivalve	0.178	0.003	16.150	0.068						
		SB1-08	Shell Bed	Bivalve	0.125	0.001	16.577	0.098						
		SB1-07	Shell Bed	Bivalve	0.250	0.005	16.504	0.105						
		SB1-06	Shell Bed	Bivalve	0.185	0.002	16.317	0.098						
		SB1-05	Shell Bed	Bivalve	0.135	0.002	16.172	0.076						
		Verzyk	upper	LL-01	Limestone Bed	Limestone	0.107	0.002			20.026	0.086	0.707812	0.000005
				FS61	Limestone Bed	Oyster	0.112	0.002			20.213	0.075		
FS45	Limestone Bed			Oyster	0.077	0.002	20.351	0.095						
LS2-06	Limestone Bed			Oyster	0.046	0.012	19.777	0.155						
LS2-05	Limestone Bed			Oyster	0.072	0.001	19.913	0.115						
lower	FS22		Shell Bed	Bivalve	0.162	0.002	16.653	0.075	0.707811	0.000006				
	FS21		Shell Bed	Bivalve	0.195	0.008	16.371	0.132						
	SB2-10		Shell Bed	Bivalve	0.153	0.027	16.241	0.289						
	SB2-09		Shell Bed	Bivalve	0.313	0.004	16.320	0.083						
	SB2-08		Shell Bed	Bivalve	0.202	0.004	16.624	0.084						
	SB2-07		Shell Bed	Bivalve	0.228	0.016	16.642	0.093						
	FS51		Shell Bed	Bivalve	0.186	0.008	15.485	0.068						
	FS32		Shell Bed	Bivalve	0.161	0.005	15.992	0.062						
	FS33		Shell Bed	Bivalve	0.192	0.002	16.638	0.089						
Karabulak	upper	SB1-10	Shell Bed	Bivalve	0.155	0.001	16.818	0.080	0.707875	0.000007				
		SB1-09	Shell Bed	Bivalve	0.154	0.001	16.678	0.080						
		LL-02	Limestone Bed	Limestone	0.116	0.002	20.487	0.090						
		FS72	Limestone Bed	Oyster	0.090	0.002	20.487	0.091						
		FS82	Limestone Bed	Oyster	0.129	0.002	20.253	0.131						
		FS71	Limestone Bed	Oyster	0.131	0.001	20.233	0.079						
	lower	LS2-07	Limestone Bed	Oyster	0.127	0.003	19.665	0.097	0.707875	0.000007				
		FS81	Limestone Bed	Oyster	0.111	0.003	19.405	0.080						
		SD-04	Shell Bed	Bivalve	0.128	0.003	15.957	0.079						
		SD-01	Shell Bed	Bivalve	0.161	0.003	16.018	0.103						
		SB2-13	Shell Bed	Bivalve	0.176	0.001	16.308	0.087						
		SB2-12	Shell Bed	Bivalve	0.241	0.025	16.705	0.087						
		SB2-11	Shell Bed	Bivalve	0.202	0.005	16.590	0.092						
		SD-03	Shell Bed	Bivalve	0.189	0.003	16.588	0.082						
SD-02	Shell Bed	Bivalve	0.171	0.007	16.776	0.153								
FS52	Shell Bed	Bivalve	0.139	0.002	16.147	0.065								
SB1-13	Shell Bed	Bivalve	0.143	0.001	16.554	0.073								
SB1-12	Shell Bed	Bivalve	0.175	0.001	16.654	0.086								
SB1-11	Shell Bed	Bivalve	0.128	0.002	16.604	0.127								

**Table 1.** The detailed table of the samples used for sulfur and strontium analysis and observed isotope values



All samples were cleaned to avoid contamination, and only the clean shell parts of the fossils and silica-free limestones were separated and powdered using an agate mortar for isotope analyses. Powdered samples (0.35–1.88 g) were processed according to a procedure modified from Maruoka and Isozaki (2020). First, powdered samples were subjected to leaching with a 30% H<sub>2</sub>O<sub>2</sub> solution at room temperature (~ 25 °C) for 24 h and at 50 °C for 24 h. This step removes organic sulfur and sulfide, which are vulnerable to oxidation. The residual sample powder was then carefully rinsed with deionized water. The H<sub>2</sub>O<sub>2</sub>-leached samples were then subjected to leaching with 10% NaCl solution for 24h. This step removed sulfates, including adsorbed evaporitic calcium sulfate and sulfates from the oxidation of sulfides. The residual sample powder was carefully rinsed with deionized water and dissolved in 6M HCl. These procedures were performed in a N<sub>2</sub>-gas atmosphere to prevent oxidation. The dissolved sulfate was precipitated as BaSO<sub>4</sub> by adding a BaCl<sub>2</sub> solution after adjusting the pH to 2–3 using a 6M KOH solution. The BaSO<sub>4</sub> precipitate was filtered using a membrane filter with a 0.2 μm pore size. The process photographs above mentioned procedures are shown in Figure 9.



**Figure 9.** The photographs of the sample preparation for isotope measurements. 1) Cleaned and powdered samples, 2) Leaching with  $H_2O_2$ , 3) Rinsing in deionized water under  $N_2$  gas atmosphere, 4) Filtering for  $BaSO_4$  residue, and 5) The ready residue of the  $BaSO_4$  for measurement.

### 3.2. Fossil Identification

Shell beds containing numerous mollusk fossils are observed in all the measured sections (Figures 3). These shell beds are densely packed with bivalves, such as oyster fossils, and several oysters corresponding to the *Pycnodonte* sp., *Liostrea* sp., *Gryphaea* (*Crassostrea*), and *Ostrea* (*Turkostrea*) genera, have been identified (Figures 10 and 11). Generally, the ages of these genera are Maastrichtian-Middle Miocene for *Pycnodonte* sp., Ladinian-Holocene for *Liostrea* sp., Ladinian-Late Eocene for *Gryphaea* (*Crassostrea*), and Maastrichtian-Middle Miocene for *Ostrea* (*Turkostrea*). However, due to the moderately long ranges of these genera, a detailed geological age cannot be assigned to the mollusk fossils. However, considering the co-occurrence of these fossils and the stratigraphy and geological examinations carried out in previous studies Abdouazimova (2011), the geological ages suggested by these fossils indicate a Late Cretaceous to Eocene.

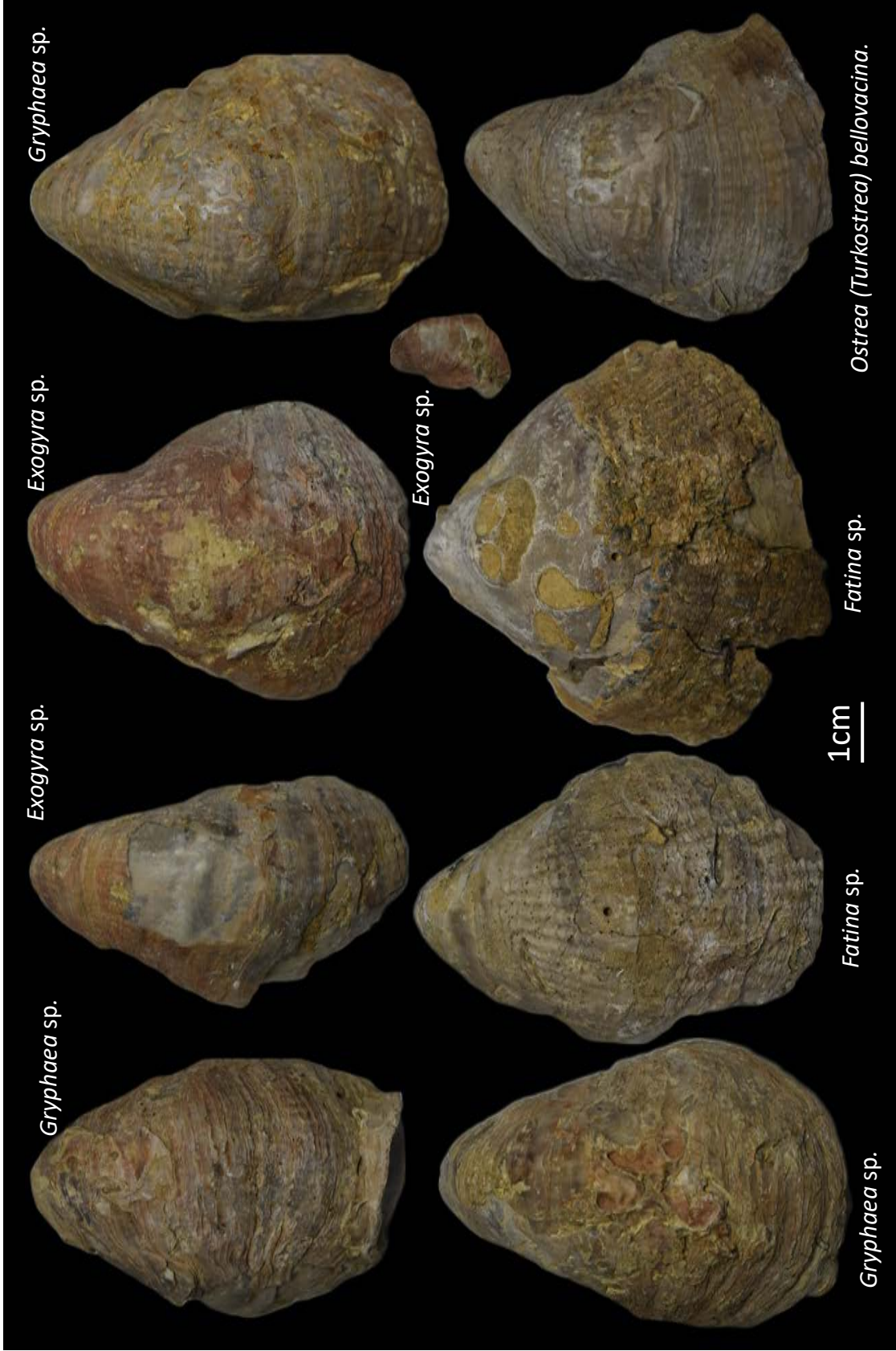


**Figure 10.** The macrofossil assemblage collected from upper sequence of the study section northern part of the Fergana Basin.

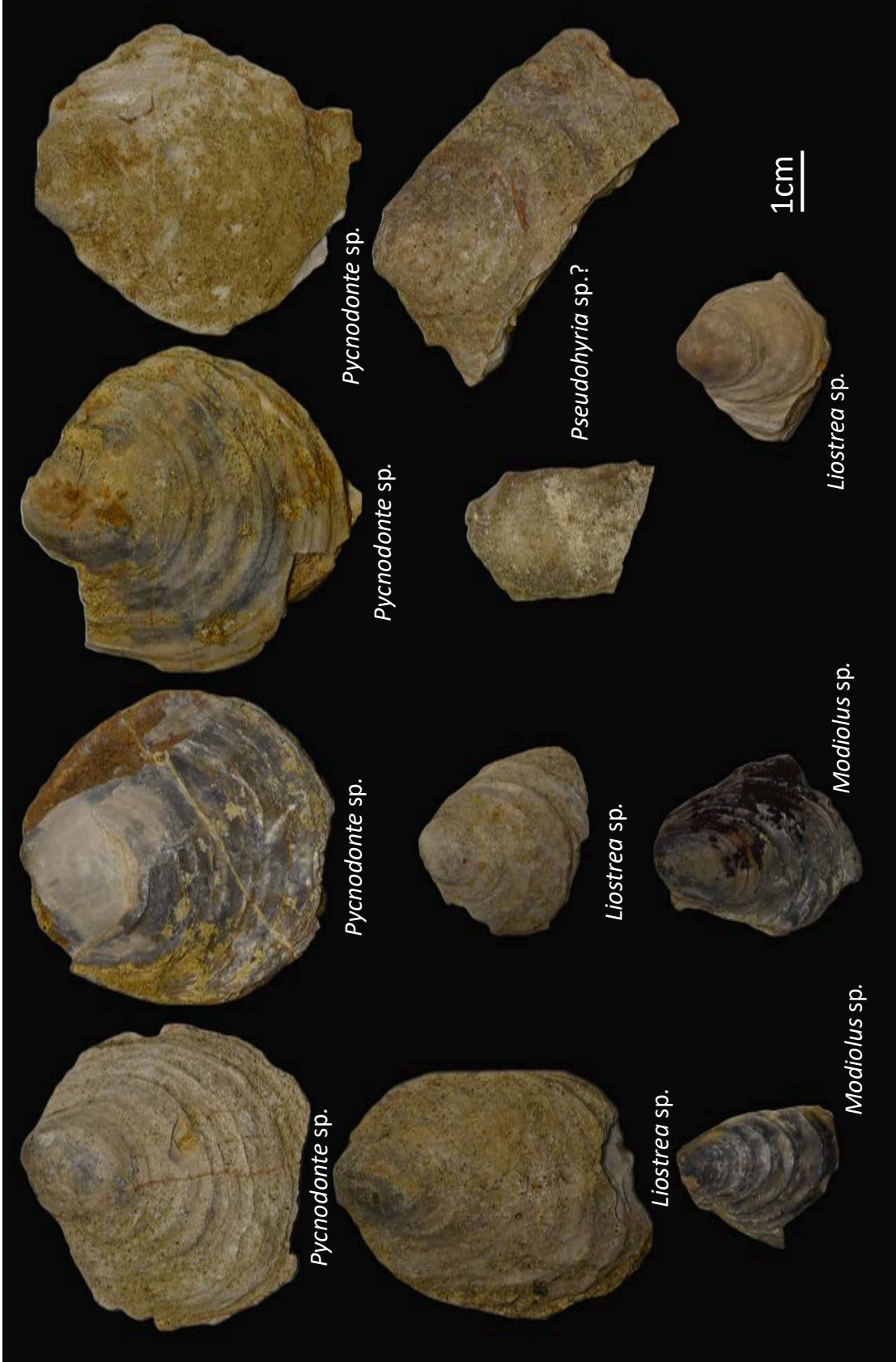


**Figure 11.** The macrofossil assemblage collected from lower sequence of the study section northern part of the Fergana Basin.

### *3.3. Stable Isotope Analysis*

#### *3.3.1. Sulfur isotope analysis of the BaSO<sub>4</sub> precipitates of the carbonate-associated sulfate*

The sulfur isotopic compositions of the BaSO<sub>4</sub> precipitates were determined using a continuous-flow isotope ratio mass spectrometer (CF-IR-MS; ISOPRIME-EA; Isoprime Ltd.) at the University of Tsukuba (Maruoka and Isozaki, 2020). Approximately 0.25 mg of the BaSO<sub>4</sub> precipitate, corresponding to 30 µg of sulfur, was weighed in a 3.3 × 5 mm tin capsule, and approximately 300 µg of V2O5 (Nacalai Tesque, Inc.) was added to promote complete combustion. Using an autosampler, the samples were introduced into a combustion/reduction quartz tube heated to 1090 °C with a helium gas flow of 90 mL/min and were then oxidized by an oxygen pulse. The combustion/reduction tube contains tungstic trioxide, which promotes complete oxidation, and pure copper wires, which remove excess oxygen and convert sulfur trioxide into sulfur dioxide. The water resulting from the combustion was removed using a magnesium perchlorate water trap. The gases produced in the combustion/reduction tube were introduced into a quartz tube containing quartz wool heated to 890 °C to minimize the oxygen isotope variation of SO<sub>2</sub> using a SO<sub>2</sub>-SiO<sub>2</sub> equilibrium reaction (Fry et al., 2002). Sulfur dioxide and other gases, such as CO<sub>2</sub> and N<sub>2</sub>, were separated via gas chromatography at 60 °C; the column used in this study was manufactured by Ludi Swiss AG (#99.0723.10). The gases were introduced into the mass spectrometer through an open-split interface.

The sulfur isotopic compositions were expressed in terms of δ<sup>34</sup>S (‰) relative to the Vienna -Canyon Diablo Troilite (V-CDT) standard. The results of two International Atomic Energy Agency (IAEA) silver sulfide standards (IAEA-S-1, -0.3‰; IAEA-S-2, +21.80‰; Mayer and Krouse, 2004) were compared to constrain the δ<sup>34</sup>S values. The isotopic compositions of sulfur were determined to a precision (1σ) of ± 0.1‰ for 30 µg

of sulfur. Precisions were determined based on a combination of standard deviations from repeated analyses of the samples and standards (Maruoka *et al.*, 2003). The sample analyses were repeated at least thrice.

### 3.3.2. Strontium isotope analysis

Out of 59 samples, 9 were chosen for Sr isotope measurements, and Sr separation for isotopic analysis was performed at JAMSTEC using a method described by Takahashi *et al.* (2009) and Kuroda *et al.* (2017). Sample powders were leached with acetic acid to decompose the carbonate fraction. Strontium was separated from other elements by using Eichrom Sr Spec resin. About 100 ng of the sample Sr was loaded on a single W filament together with Ta activator. Sr isotopic ratios were measured by static multi-collection mode using Thermo Scientific TRITON thermal ionization mass spectrometer at Kochi Core Center following the method described in (Wakaki *et al.*, 2018). A measurement consists of 140 cycles of 16.8 s integrations with  $^{88}\text{Sr}$  ion beams of 4V. Instrumental mass fractionation was corrected to  $^{86}\text{Sr}/^{88}\text{Sr} = 0.1194$  using exponential law. Baselines of the faraday cup detectors were measured for 300 s just before each of the measurement. The average  $^{86}\text{Sr}/^{88}\text{Sr}$  ratio of NIST SRM 987 was  $0.710247 \pm 0.000013$  (2SD, n = 5).  $^{86}\text{Sr}/^{88}\text{Sr}$  ratio of the sample was corrected to  $^{86}\text{Sr}/^{88}\text{Sr}_{\text{SRM 987}} = 0.710248$  (McArthur *et al.*, 2012) using this measured value.



#### 4. Results

As presented in Table 1 and Figure 12A, the sulfur isotopic compositions ( $\delta^{34}\text{S}$ ) of the measured fossil shells from the sandstone shell beds of the lower sequence are between 14.94 and 16.82‰. In addition, the  $\delta^{34}\text{S}$  values for the limestone and fossils from the lower sequences of the four sections range between 19.37 and 21.19‰, which deviates from the result obtained for the sandstone shell beds. Furthermore, the  $^{87}\text{Sr}/^{86}\text{Sr}$  ratios of the bivalve fossil samples from the lower sequence range between 0.707772 and 0.707875 (Table 1, Figure 12B), whereas the  $^{87}\text{Sr}/^{86}\text{Sr}$  ratios of the upper sequence samples range between 0.707812 and 0.708063 (Figure 12B).

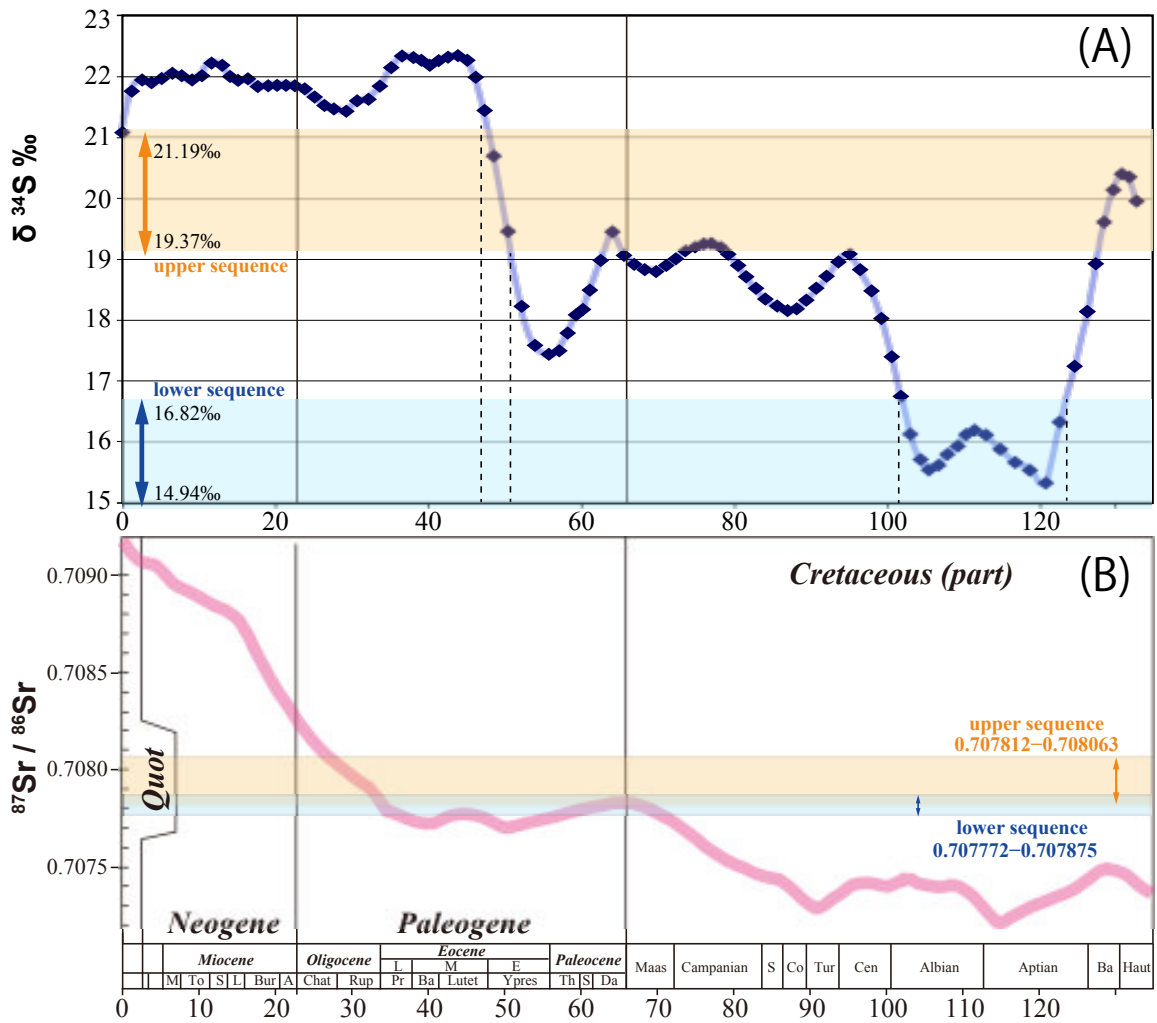


**Figure 12.** The LOWESS curve of the sulfur and strontium isotopic values for the last 130 million years. The sulfur isotopic compositions (A) were obtained from Paytan (2004), and the Sr isotopic compositions (B) were obtained from McArthur (2012, 2020). The tangents between the sulfur isotope value obtained in this study and the LOWESS curve allowed for the determination of the geological age (A).

## 5. Discussions

### 5.1. Stratigraphy

The regional stratigraphy and lithological features distributed in the northern part of the Fergana Basin are characterized by various clastic rocks intercalated with several horizons of limestone beds. The clastic rocks of the studied sections predominantly comprise intercalated red mudstone and sandstone with several beds of conglomerate. As mentioned above, reddish mudstone often contains caliches and is interpreted as terrestrial sediment. The inclusion of caliche indicates that its red beds are of terrestrial origin (Horiuchi *et al.*, 2012).

These lithofacies, composed of intercalated red mudstone and sandstone with conglomerate, indicate terrestrial deposits. Two or three beds of limestone contain mollusk fossils represented by oysters. As mentioned above, these limestone beds contain many bioclastics, including gastropods, bivalves, foraminifers, and oolite grains. The microscopic texture and these contents indicate that the limestone is of shallow-marine origin. These limestone beds, in their color as well as marine beds, contrast with the surrounding terrestrial beds and are favorable landmarks from a geological correlation perspective. This line of evidence indicates that the sedimentary beds of the study sections should be correlated with a sequence of rocks reported as the Fergana Group from Kyrgyzstan by Bande *et al.* (2017) and Bosboom *et al.* (2017). In particular, the limestone-clastic sequence is correlated with FA4 of the Fergana Group, based on lithological sequence (Bande *et al.*, 2017). Mollusk fauna from shell beds associated with marine limestone beds are dominated by oysters (Figure 3, 10 and 11). This type of marine fauna within the terrestrial reddish facies has been reported in the proto-Paratethys sediments of the Afghan-Tajik and Trim basins. Although a few bivalves were identified in this study, their dense occurrence and predominant oysters in this fauna

indicate that the limestone beds with the shell bed can be broadly correlated (Table 2). The geological correlation indicates that the limestone beds distributed in the northern Fergana Basin, Eastern Uzbekistan, were a product of the incursion of the proto-Paratethys Ocean (e.g., Bosboom *et al.*, 2017; Bande *et al.*, 2017).

Alai Valley Basin and Fergana Basin (Kyrgyzstan)					This study (Fergana Basin, Uzbekistan)		
System	Formation	Thickness (m)	Age	Lithology	seq.	Thickness (m)	Lithology
Palaeogene	Massaget Fm		Oligocene –Miocene	Massive red sandstones and conglomerates			
	Shurysay Fm	20–160	Oligocene	Brownish red-mudstones intercalated by siltstones, evaporite beds and sandstones			
	Sumsar Fm	0–70	Late Eocene –Oligocene	Reddish-brown mudstones and grey sandstones rich in oysters and other bivalves, shark teeth			
	Hanabad Fm	5–70	Late Eocene –Oligocene	Greenish-grey and red (calcareous) mudstones and siltstones, some marls with bivalves			
	Isfara Fm	5–55	Late Eocene	Greenish-grey (calcareous) mudstones and siltstones, some green or white sandstones, some marls with bivalves			
	Rishtam Fm	5–60	Late Eocene	Red mudstones with thin beds of red or grey siltstone and sandstone, some interbeds of marl and limestone with bivalves			
	Turkestan Fm	5–150	Middle–late Eocene	Greenish-grey mudstones with grey and white siltstones, sandstones, marls and limestones, red mudstone intervals at the top, rich in oysters and other bivalves	upper sequence	30–50	red mudstones with sandstones, several limestone beds, rich in oysters
	Alai Fm	10–210	Middle Eocene	Greenish-grey mudstones with grey and white siltstones, marls and limestones, some gypsiferous red mudstone intervals in middle, rich in oysters and other bivalves			
	Suzak Fm	5–120	Early Eocene	Complex coloured (calcareous) mudstones, siltstones and sandstones, bivalves	? lower sequence	5–30	reddish- and greenish-color mudstones, sandstone shell beds, bivalves
	Bukhara Fm	20–80	Paleocene	Limestones, evaporite beds and white sandstones with thin calcareous mudstone layers, bivalves and gastropods			
	Akdzhar Fm	25–125	Paleocene	Red mudstones and siltstones with interbeds of evaporite and dolomite			

**Table 2.** The simplified lithostratigraphy and geological correlations of the studied sections with the stratigraphy and lithology of the Alai Valley Basin and the Fergana Basin (Kyrgyzstan) which were obtained from Bosboom *et al.*, (2017).

## 5.2. Geochronology

The sulfur isotopic composition of dissolved sulfate in seawater varies with geological time, and sulfur isotope records include data sets from the Cambrian to the present (e.g., Claypool *et al.*, 1980; Strauss, 1997; Kampschulte and Strauss, 2004). Its variation and moderately high rates of change show distinctive excursion curves and characterize certain time intervals in geological time (e.g., Surakotra *et al.*, 2018). Owing to these properties, it is possible to make geological correlations and determine the geological age of sediments using sulfur isotopes (e.g., Paytan *et al.*, 2012; 2020). From the Cretaceous to the Cenozoic, high-resolution sulfur isotope excursion was restored based on barite within precisely age-determined core sediments (Paytan *et al.*, 1998; 2004). A sulfur isotope curve was obtained from pelagic marine barites of Cretaceous and Cenozoic ages, with unprecedented temporal resolution (Paytan *et al.*, 1998, 2004). These results generally agree with those obtained from carbonate-associated sulfates in carbonate sediments (Kampschulte and Strauss, 2004). As mentioned above, since the sulfur isotope ratio curve from the Cretaceous to the Cenozoic is effective for age dating, we will discuss age determination based on the sulfur isotope ratios obtained in this study.

The S isotope compositions obtained in this study are listed in Table 1 and Figure 12. Sulfur isotopic compositions were divided into two groups; one of them was relatively lower than the other group and falls in the 14.94–16.82‰ range, which was obtained from the sandstone shell bed consisting of the underlying sequence of the lower part of the studied sections. The other group ranges from 19.37‰ to 21.19‰ and was obtained from fossil shells and limestone containing the limestone-clastic sequence of the studied sections, as shown in Figure 3.

As mentioned in the chapter on fossil occurrence, the mollusk fossils broadly indicate the interval from the Late Cretaceous to the Eocene.

Based on the Cretaceous to present sulfur isotopic curve summarized by Paytan *et al.* (2020), the isotopic composition of the limestone-clastic sequence corresponds to a steep slope part of approximately 50–45 Ma (Figure 12). This part is the period when the sulfur isotope ratio rises rapidly and corresponds to the Early to Middle Eocene. In addition to the range of sulfur isotope ratios, the increasing trend of  $\delta^{34}\text{S}$  values from the lower layer to the upper layer (e.g., from 19.44 to 21.19 for the Gava 1 section) also supports this age assignment. Higher isotopic values ranging from 19.37‰ to 21.19‰ are observed in the lowest Cretaceous in the isotope curve; however, it should be assigned to the 50–45 Ma part of the Early to Middle Eocene, considering the mollusk range.

In contrast, the low values (14.94 ‰ and 16.82 ‰) obtained from the underlying sequence are like those of the Early Cretaceous (approximately 120 and 100 Ma) when the sulfur isotope ratio was extremely low. However, considering the range of mollusk fossils, it is difficult to assign them to the Early Cretaceous. Unconformities and eroded surfaces that indicate a large time gap were not observed between the limestone-clastic sequence and the underlying sequence. The lithology and fossil contents of the limestone beds comprising the limestone-clastic sequence indicate a shallow marine origin. In contrast, numerous clastics consisting of the underlying sequence indicates that it might be affected by terrestrial sedimentation and fresh water. It is possible that this supply of terrestrial water recorded a sulfur isotope ratio lower than that of seawater at that time. This is because the sulfur isotope ratios of seawater are higher than those of any of the input sources to the oceans, owing to the removal of low  $\delta^{34}\text{S}$  sulfur from seawater through bacterial sulfate reduction (Kaplan and Rittenberg, 1964). In addition, although

unlikely, the reworking of the bivalves could not be excluded as a cause of the isotopic compositions.

In addition to the S isotope, the Sr isotope composition was measured in this study. The Sr isotopic compositions of the measured samples are 0.707812–0.708063 at the underlying sequence and 0.707772–0.707875 at the limestone-clastic sequence and are approximately equal (Table 1, Figure 12). These Sr isotopic compositions are equivalent to the Paleogene value of the LOWESS (LOcally WEighted Scatterplot Smoothing) curve reported by McArthur *et al.*, (2012; 2020) (Figure 12). The result of the strontium isotope ratio does not exactly concordant with the geological age indicated by the sulfur isotope ratio. But since it is closer to the value of the Paleogene than that of the Cretaceous, the strontium isotope ratio seems to support our interpretation on the geological age estimation based on the S isotope. However, just as the effects of freshwater and terrestrial materials have been suggested on the sulfur isotope ratios. According to the McArthur (1992) the supplement of the strontium to the world oceans are carried out by three procedures: 1) the hydrothermal circulation through hot rocks, which is the primary source of the Sr ( $^{87}\text{Sr}/^{86}\text{Sr}$ : 0.704), 2) recrystallization of carbonate sediments during burial ( $^{87}\text{Sr}/^{86}\text{Sr}$ : 0.708), and 3) by terrestrial rivers and streams ( $^{87}\text{Sr}/^{86}\text{Sr}$ : 0.712). According to the observed lithology, the study area shows the transition from terrestrial to marine environment, and therefore, it is proper to conclude that the supplement of the strontium to the sediments were brought by the freshwaters by rivers and streams (Figure 13). Additionally, in the previous chapter, in the lesser part of the Gava and Varzyk sections the several structures which indicates the river structures such as trough cross beddings were observed, and this is the evidence of the existence of the rivers which flowed to the sea carrying the strontium isotopes.



As mentioned above, the sections in this study are characterized by large amounts of terrestrial and reddish clastics and the intercalation of two or three marine limestone beds. These stratigraphy and lithology are very similar to those of the Fergana Formation, which has been assigned to the Early to Middle Eocene (Bande *et al.*, 2017). Because the Cenozoic sedimentary rocks distributed in the Fergana Basin occupy a large number of terrestrial sediments, it is difficult to precisely determine the geological age. In this study, the depositional age was estimated using mollusks and two isotopic compositions (S and Sr), but further studies using microfossils such as foraminifera are required.

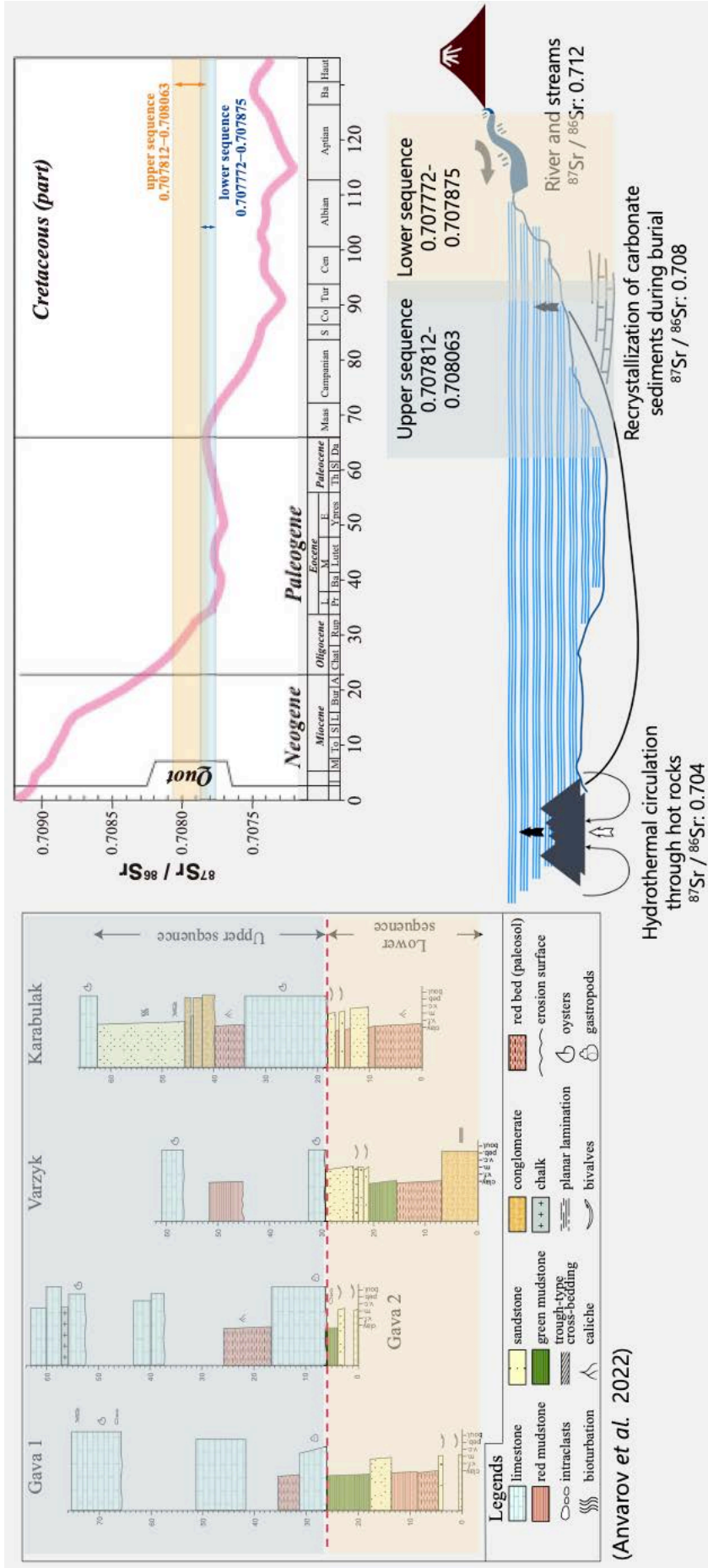


**Figure 13.** The illustration of the Sr (strontium) supply to the world oceans adopted by McArthur (1992) and modified to the northern part of the Fergana Basin. Here, the obtained Sr value from lower sequence was higher than those applied for world oceans LOWESS curve and suggesting the supply of the strontium were mainly from river and stream freshwater. On the other hand, the upper sequence Sr value is concordant to the LOWESS curve of world oceans crossing the line between the Eocene interval, suggesting there were no effect of the freshwater, and Sr was supplied recrystallization of carbonate sediments during the burial.

### 5.3. The Fourth Marine Incursion of the paleo-Paratethys

Mesozoic and Cenozoic sediments distributed in the Fergana Basin, along with rocks from the Afghan-Tajik and Tarim basins, were targeted to examine the extent of the proto-Paratethys Ocean in Central Asia. As mentioned above, the lithology and stratigraphy of the studied sections, contents of mollusk fossils, and depositional ages by S and Sr isotope compositions indicate that the study sections should be assigned to the 50–45 Ma part of the Early to Middle Eocene. Recently, Bosboom *et al.* (2011) and Bosboom *et al.* (2017) investigated lithostratigraphy and depositional ages of the Cretaceous to Paleogene distributed in the southern part of the Fergana Basin and reviewed its equivalent sequences distributed in the Afghan-Tajik Basin and Alai Valley Basin. This series of studies has established a detailed geological correlation of the sequence among the basins in Central Asia and clarified the transitions of the proto-Paratethys Ocean in the Cretaceous to Paleogene, which was five transgression and regression. The third is considered the largest (Tang *et al.*, 1989; Lan and Wei 1995; Burtman *et al.*, 1996; Burtman 2000), and the peak of the fourth transgression has been estimated to be around the Middle Eocene (Lutetian) (Bosboom *et al.*, 2011, 2014). Two or three limestone beds in the study sections have S and Sr isotopic values equivalent to those of the Early to Middle Eocene (ca. 50–45 Ma) of the LOWESS curve (Figure 12). In addition to the estimated depositional age by S and Sr isotopes, microscopic features that are characterized by shallow-water indicators such as oolite and cortoid grains indicate that the limestone beds should correspond to the stage of the fourth transgression of the proto-Paratethys Ocean in the study area. Sandstone shell beds of the underlying sequence densely yield oyster shells and consist mainly of angular and poorly sorted quartz grains. Because the sulfur isotope ratio indicates the influence of freshwater, it is predicted that the shell beds correspond to the intertidal deposits. The transition from

the terrestrial 'lower sequence' to the marine 'upper sequence' in the study sections may represent the fourth transgression stage of the proto-Paratethys Ocean in the Early to Middle Eocene in the northern Fergana Basin.

## 6. Conclusions

Lithostratigraphy of the limestone-clastic sequence, which consists mainly of red terrestrial clastic and shallow marine limestone, is described in the northern Fergana Basin, Eastern Uzbekistan. Two or three shallow marine limestone beds were intercalated with red mudstone, coarse-grained sandstone, and conglomerate.

Macrofossils represented by bivalves, such as oysters, were obtained from sandstone shell beds of the underlying sequence in the lower section and limestone beds of the limestone sequence in the upper section.

Sulfur isotope values of the limestone beds of the limestone-clastic sequence indicate a moderately high sulfur isotopic composition in the 19.37–21.19‰ range. Conversely, the Sr isotopic compositions of the measured samples are 0.707812–0.708063 at the underlying sequence and 0.707772–0.707875 at the limestone-clastic sequence.

Sulfur isotopic composition of the shell bed consisting of the underlying sequence has a moderately low composition, ranging from 14.94 ‰ to 16.82 ‰. Tangents between this isotopic composition and LOWESS curves indicate Early Cretaceous age; however, it is possible that the isotope composition recorded different values from seawater at the time owing to the terrestrial clastics and water (fresh water) effect. Determining the age of the underlying sequence requires further studies.

Lithofacies and age determination of the limestone-clastic sequence indicate that the limestone beds can be correlated with FA4 of the Fergana Group of Bosboom *et al.* (2017), which is representative horizons of the fourth transgression of the proto-Paratethys Ocean.

The line of evidence, such as lithofacies, macrofossil contents, geological correlation, and age determination by S and Sr isotopic compositions, indicates that the

limestone beds distributed in the northern Fergana Basin are remnants of the fourth transgression of the proto-Paratethys during the Eocene.

## **Acknowledgements**

It was very hard last years of my study and research of Ph.D. degree, but the advices, suggestions and mental cheering of my supervisor Prof. Yoshihito KAMATA gave me much more power to fulfil my dream on getting degree. Without him it was impossible to publish my paper and write this thesis. Thank you very much for every single effort you made towards me.

My sincere gratitude and heartfelt appreciations to my former supervisor Prof. Ken-ichiro HISADA for his entire support, advice and everything he did not only for me but also to my family. It is simply impossible my life here without his advices and support not only in academic but also in personal life. With his agreement and support on doing research in my country and connect two countries my motherland Uzbekistan and fatherland Japan, I am standing here and writing my thesis, published my paper and achieved everything related to my dream. Following, heartfelt gratitude towards Mrs. Kazue HISADA for being for us here or in a short being our mother here. I simple do not have enough words to express my gratitude towards her.

I would like to thank every single person who was involved in my journey of getting this degree for their sincere support and advice. My sincere gratitude towards all professors of our faculty whose door of their office were always open for me. I would like to thank Prof. Teruyuki MARUOKA for his great effort on isotope analysis, his suggestions and for most time being a friend of mine. I still remember that you said: "Let's be friends and it will be easier to get along, rather than professor-student relationship".

My sincere acknowledgements due to Prof. Shigehiro FUJINO and Prof. Kaoru SUGIHARA for their valuable suggestions and sincere support in my studies. They gave

the most important and critical advices during not only laboratory seminars but also in daily basis.

Hereinafter, I want to express my heartfelt appreciations and gratitude towards special persons: Prof. Kohei TANAKA, Prof. Yoshitsugu KOBAYASHI of Hokkaido University and my dear friend Mr. Sherzod MAKHMUDOV for their acceptance my crazy ideas and dreams on connection of two countries in science. Without their agreement and support this study will not be happened.

My special acknowledgements due to Prof. Thomas PARKNER who was the first person who opened the doors of geoscience and showed the wonders of it. I will never forget his kindness, support and advices.

If I count every single person, it will be longer than this thesis in general. Simply but sincerely would like to thank everyone whom I met in my journey and get along with. Especially, Dr. Kohei TOMINAGA (Tomi – my real friend), Mr. Shogo ISHII (Ishii-san, as my daughter used to call), Dr. Masaki YAMADA (my daughter's best friend and uncle), Prof. Ryo OKUWAKI, Prof. Atsushi KYONO and Ms. Yuki TAKANO (my dearest sister and best friend of my family) for being best friend of mine and giving me an unforgettable memory of my student life.

Last, but not least I would like to express my sincere gratitude to TAKAYAMA International Educational Foundation for their support with scholarship which was one of the most important to achieve my dreams on research in my country. I thank all the members and professors for their trust for me and support on everything.

Finally, I would like to thank my family, my father and mother for giving me the chance to study abroad, support my decisions and for every single attribution they made till now and now on then. My endless appreciation towards my brother and sister who is supporting and caring my parents while I am far from home and for their patience and



support. I thank my little family my lovely wife (never said this to her), my precious daughter (the apple of my eye) and my brave son (he will be the greatest football player in future) for their patience, support and everyday warmth that gives me power to move on to achieve my goals. Thank you, my dears and be healthy for me.

I believe, every single situation in my life, every single person, every single good and bad days were gifted to me by God (ALLAH) and I my gratitude and appreciations are till the end of my life. It is hard to explain and simply say thanks but he the one who knows everything.

Thank you very much for all and my endless respect towards you.

I dedicate this work to the sweet memory of my lovely grandfather, may he rest in peace, Amin.

## References

- Abduazimova, I. M., Bogomolova, A. M., Shevtsova, E. M. The Correlation of the Aptian and Albian of the Central Kyzylkum and South-western foothills of the Gissar Range. Geol. J. of Uzb. 1984, No. 2, pp. 59–61. (in Russian).
- Abduazimova, I. M., Shevtsova, E. M. The formations of the Lower Cretaceous deposits of the Central Kyzylkum. Geol. J. of Uzb. 1987, No. 3, pp. 54–57. (in Russian).
- Abduazimova, I. M., Shevtsova, E. M. The Aksagata Formation – new stratigraphic unit of the Upper Cretaceous of the near Tashkent Mountain areas. Geol. J. of Uzb. 1988, No. 4, pp. 67–68. (in Russian).
- Abduazimova, I. M., Kim, A. I., Meshankina, N. A., Bogomolova, A. M. The atlas of the fauna and flora of the Phanerozoic of Uzbekistan. The Mesozoic and Cenozoic (Jurassic, Cretaceous and Paleogene). Tashkent, StateGeolCom. Pub. RUz., 2007, Vol. 2, pp. 76–135. (in Russian).
- Abduazimova, I. M.; Kan, O. Yu. The stratigraphy and paleogeography of the Cretaceous Fergana Depression by new case studies Part 1: Stratigraphy. The J. of Geol. and Min. Res., 2012, 5, pp. 3–12. (In Russian).
- Abduazimova, I. M.; Kan, O. Yu. The stratigraphy and paleogeography of the Cretaceous Fergana Depression by new case studies Part 2: Paleogeography. The J. of Geol. and Min. Res., 2012, 6, pp. 3–10. (In Russian).

Abdullayev, R. N., Dalimov, T. N., Mukhin, P. A. and Bazarbaev, E. R. Rifting in the development of the Paleozoic folded regions. Tashkent, Fan, 1989, 112 pp (in Russian).

Akhmedjanov, M. A., Borisov, O. M. and Fuzailov, I. A. The structure and composition of the Paleozoic basement of Uzbekistan. Tashkent, Fan, 1967, 162 pp (in Russian).

Allen, M. B., B. F. Windley, and C. Zhang. Palaeozoic collisional tectonics and magmatism of the Chinese Tien Shan, Central Asia, *Tectonophysics*, 1992, 220, 89–115.

Alferov, G. Yu. The stratigraphy of the Neogene deposits of the Western Uzbekistan. The paleontological justification of the Mesozoic and Cenozoic sediments of Uzbekistan. Tashkent: Fan, 1969, pp. 165–195. (in Russian).

Alferov, G. Yu. Bunyak, L. I., Kurbatov, V. V., Derevyanko V. I. Paleogeographic and tectonic criteria on the establishing and estimating the Upper Cretaceous reef complexes with example of Southern Uzbekistan. The methods of searching and expediting the cellar reefs. Moscow: Nauka, 1983, pp. 67–70. (in Russian).

Anvarov, O.U.O.; Kamata, Y.; Maruoka, T.; Kuroda, J.; Wakaki, S.; Hisada, K.-i. Paleogene Lithostratigraphy and Recognition of the Marine Incursion of the Proto-Paratethys Sea in the Fergana Basin, Uzbekistan. *Geosciences* 2022, 12, 203. <https://doi.org/10.3390/geosciences12050203>.

Arkhangelskiy, A. D. The Upper Cretaceous Deposits of Turkestan. Part I. The Upper Cretaceous Deposits of north-western Kyzylkum and Fergana. Geol. Com. Research, New editions, 1916, Vol. 151. (in Russian).

Arkhangelskiy, A. D. Geological structures of USSR. Moscow, Grozniy, Leningrad, Novosibirsk: Mounoilpub, 1934, Vol. I 224 pp.; Vol. II 428 pp. (in Russian).

Averianov, A.O, Sues, H-D. Skeletal remains of Tyrannosauroida (Dinosauria: Theropoda) from the Bissekty Formation (Upper Cretaceous: Turonian) of Uzbekistan. Cret. Res. 2012, 34, 284–297. (doi:10.1016/j.cretres.2011.11.009).

Askarov, F.A.; Bigaeva, A.R.; Saydyganiev, S.S. Absolute Geochronology of the Magmatic Formations of Uzbekistan; FAN UzSSR; Publications of Academy of Sciences UzSSR: Tashkent, Uzbekistan, 1974; pp. 127–134. (In Russian).

Bande, A.; Radjabov, S.; Sobel, E.D.; Sim, T. Cenozoic palaeoenvironmental and tectonic controls on the evolution of the northern Fergana Basin. In Geological Evolution of Central Asian Basins and the Western Tien Shan Range; Brunet, M.-F., McCann, T., Sobel, E.R., Eds.; The Geological Society of London, Special Publications: London, UK, 2017; Volume 427, pp. 313–335.

Biske, Y. S. Island arcs in the Paleozoic history of Southern Tien Shan. Geotectonika, 1991, 2, pp. 6–41. (in Russian).

Bosboom, R.E.; Dupont-Bosboom, R.; Mandic, O.; Dupont-Nivet, G.; Proust, J.-N.; Ormukov,

C.; Aminov, J. Late Eocene palaeogeography of the proto-Paratethys Sea in Central Asia (NW China, southern Kyrgyzstan and SW Tajikistan). In Geological Evolution of Central Asian Basins and the Western Tien-Shan Range; Brunet, M.-F., McCann, T., Sobel, E.R., Eds.; Geological Society of London, Special Publications: London, UK, 2017; Volume 427, pp. 565–588.

Bosboom, R.E.; Dupont-Nivet, G.; Houben, A.J.; Brinkhuis, H.; Villa, G.; Mandic, O.; Stoica, M.; Zachariasse, W.J.; Guo, Z.; Li, C.; et al. Late Eocene sea retreat from the Tarim Basin (West China) and concomitant asian paleoenvironmental change. *Palaeogeogr. Palaeoclimatol. Palaeoecol.* 2011, 299, 385–398.

Bosboom, R.E.; Dupont-Nivet, G.; Grothe, A.; Brinkhuis, H.; Villa, G.; Mandic, O.; Stoica M.; Huang, W.; Yang, W.; Guo, Z.; Krijgsman, W. Linking Tarim Basin sea retreat (west China) and Asian aridification in the late Eocene. *Basin Res.* 2014, 26, 621–640.

Burtman, V.S.; Molnar, P. Geological and Geophysical Evidence for Deep Subduction of Continental Crust Beneath the Pamir; Special Papers; GSA: Boulder, CO, USA, 1993; Volume 281.

Burtman, V.S.; Skobelev, S.F.; Molnar, P. Late Cenozoic slip on the Talas-Fergana Fault, the Tien Shan, Central Asia. *GSA Bull.* 1996, 108, 1004–1021.

Chernyshev F. N., Bronnikov, M. M., Verber, V. N., and Faas, A. V. The Andijan Earthquake. Turkestan, Pub.GeolCom. 1910, Vol. 54. (in Russian).

- Claypool, G.E.; Holser, W.T.; Kaplan, I.R.; Sakai, H.; Zak, I. The age curves of sulfur and oxygen isotopes in marine sulfate and their mutual interpretation. *Chem. Geol.* 1980, 28, 199–260.
- Coplen, T.B.; Krouse, H.R. Sulphur isotope data consistency improved. *Nature* 1998, 392, 32.
- Fry, B.; Silva, S.R.; Kendall, C.; Anderson, R.K. Oxygen isotope corrections for online  $\delta^{34}\text{S}$  analysis. *Rapid Commun. Mass Spectrom.* 2002, 16, 854–858.
- Glumakov, P.V. Fergana Depression. In *Tectonics, Formation, and Oil-Gas Depositions of the Intermountain Basins*; Nauka: Moscow, Russia, 1988; pp. 5–39. (in Russian).
- Horiuchi, Y.; Charusiri, P.; Hisada, K. Identification of an anastomosing river system in the Early Cretaceous Khorat Basin, northern Thailand, using stratigraphy and paleosols. *J. Asian Earth Sci.* 2012, 61, 62–77.
- Jarnilskaya, G. I. The new Cretaceous gastropods from lacustrine and lagoon deposits of the Southern and Eastern Fergana. Chapter from: *The Cretaceous continental deposits of the Fergana*. Moscow: Nauka, 1965, pp. 140–148. (in Russian).
- Jolivet, M. Mesozoic tectonic and topographic evolution of Central Asia and Tibet: A preliminary synthesis. In *Geological Evolution of Central Asian Basins and the Western Tien-Shan Range*; Brunet, M.-F., McCann, T., Sobel, E.R., Eds.; Geological Society of London, Special Publications: London, UK, 2017; Volume 427.

Kampschulte, A.; Strauss, H. The sulfur isotopic evolution of Phanerozoic seawater based on the analysis of structurally substituted sulfate in carbonates. *Chem. Geol.* 2004, 204, 255–286.

Kaplan, I.R.; Rittenberg, S.C. Microbiological fractionation of sulfur isotopes. *J. General Microbiology* 1964, 34, 195–212.

Keshishyan, K. A., Abduazimova, Z. M., Tabachenko, L. M. The content of the working legend-50 mountains of Sultanuizdag. Tashkent, State. Com. Geol., 1995. (in Russian).

Kurenkov, S. A. Tectonics of ophiolite complexes of Southern Tien Shan. Moscow: Nauka. 1983, 100 pp. (in Russian).

Kuroda, J.; Hara, H.; Ueno, K.; Charoentitirat, T.; Maruoka, T.; Miyazaki, T.; Miyahigashi, A.; Lugli, S. Characterization of sulfate mineral deposits in central Thailand. *Island Arc* 2017, 26, e12175.

Lan, X.; Wei, J. Late Cretaceous-Early Tertiary Marine Bivalve Fauna from the Western Tarim Basin; China Sci. Press: Beijing, China, 1995; pp. 1–212.

Maruoka, T.; Koeberl, C.; Matsuda, J.; Syono, Y. Carbon isotope fractionation between graphite and diamond during shock experiments. *Meteorit. Planet. Sci.* 2003, 38, 1255–1262.

Maruoka, T.; Isozaki, Y. Sulfur and carbon isotopic systematics of Guadalupian-Lopingian (Permian) mid-Panthalassa:  $\delta^{34}\text{S}$  and  $\delta^{13}\text{C}$  profiles in accreted paleo-atoll carbonates in Japan. *Island Arc* 2020, 29, e12362.

Mayer, B.; Krouse, H.R. Procedures for sulfur isotope abundance studies. In *Handbook of Stable Isotope Analytical Techniques*; de Groot, P.A., Ed.; Elsevier: Amsterdam, The Netherlands, 2004; Volume 1, pp. 538–596.

McArthur, J. M., Kennedy, W.J., Gale, A.S., Thirlwall, M.F., Chen, M., Burnett, J. and Hancock, J.M. Strontium-isotope stratigraphy in the Late Cretaceous: intercontinental correlation of the Campanian/Maastrichtian boundary. *Terra Nova* 4, 385–393, 1992.

McArthur, J.M.; Howarth, R.J.; Shields, G.A. Strontium Isotope Stratigraphy. In *The Geologic Time Scale 2012*, 1st ed.; Gradstein, F.M., Ogg, J.G., Schmitz, M.D., Ogg, G.M., Eds.; Elsevier: Amsterdam, The Netherlands, 2012; Volume 1, pp. 127–144.

McArthur, J.M.; Howarth, R.J.; Shields, G.A.; Zhou, Y. Strontium Isotope Stratigraphy. In *The Geologic Time Scale 2020*, 1st ed.; Gradstein, F.M., Ogg, J.G., Schmitz, M.D., Ogg, G.M., Eds.; Elsevier: Amsterdam, The Netherlands, 2020; Volume 1, pp. 211–238.

Mirkamalov, R.H. Geological map of the Republic of Uzbekistan (1:2,500,000). In *Atlas of the Geological Maps of the Republic of Uzbekistan*; Turamuratov, I.B., Mirkamalov,



R.H., Eds.; Research Institute of Mineral Resources (RIMR): Tashkent, Uzbekistan, 2016; pp. 18–19. (in Russian).

Mirkamalov, R. X., Mukhin, P. A. and Egamberdiev, S. A. The paleomagnetism of the Kulkuduk unit in the Tamdytau ridge (Kyzylkum) in 4<sup>th</sup> All Union Geomagnetic Conference. Abstracts, Part 2, Vladimir-Suzdal, AN USSR, 1991a, pp. 142–143. (in Russian).

Mirkamalov, R. X., Mukhin, P. A. and Egamberdiev, S. A. Paleomagnetic data of the Kokpatas unit in the Kuljuktau ridge (Kyzylkum). in 4<sup>th</sup> All Union Geomagnetic Conference. Abstracts, Part 2, Vladimir-Suzdal, AN USSR, 1991b, pp. 169–170. (in Russian).

Mikhaylov, V. V. Atlas of the geological maps of the Republic of Uzbekistan. By Turamuradov I. B., Mirkamalov R. X. and others. StateGeolCom. RUz., 2016, pp 134. (in Russian).

Mukhin, P. A., Abdullaev, Kh. A., Minaev, E. V. Paleozoic geodynamics of Central Asia. Int. Geol. Rev., 1989, 31(11), pp. 1073–1083.

Mukhin, P. A., Fedeicheva, L. P. and Domoryad, A. V. The petrological peculiarities of the Paleozoic spreading zones of the Kyzylkum desert, in The Geology and Geodynamics of the Kyzylkum-Turkestan area. Tashkent: SAIGIMS, pp. 51–63. (in Russian).

Mushketov, I. V. Turkestan. The geological and orographically description by the data collected during expedition from 1874 to 1880. 1886, ScPb. (in Russian).

Mushketov, I. V. Turkestan. Vol. 2. 1906, ScPb. (in Russian).

Mushketov, V. I. Eastern Fergana. Pub. Geol. Commeette. 1911, Vol. 30, No. 10. (in Russian).

Mushketov, V. I. The geological outlines of the Eastern Fergana. Pub. ScPb. NatSci. 1912, Vol. 43, No. 1. (in Russian).

Mushketov, V. I. Alayku. The summary of the geological expeditions to Eastern Fergana in 1912. Pub. Geol. Commeette. 1913, Vol. 32, No. 7. (in Russian).

Mushketov, V. I. The Geological Map of the Central Asia. Part I. Lists: IV-7 and VII-7 (Eastern Fergana). Pub. Geol. Commeette. New sereies. 1928, Vol. 169. (in Russian).

Nalivkin, D. V. The geological outline of Turkestan. Pub.: Turkpechat', Tashkent, 1926. (in Russian).

Nalivkin, D. V. Geology of USSR; Publications of the Academy of Science USSR: Moscow, Russia, 1962. (in Russian).

Nesov, L.A. Dinosaurs of northern Eurasia: New data about assemblages, ecology

and paleobiogeography. Pub. of Sankt-Peterburg University,  
Saint Petersburg, 1995. (in Russian).

Nesov, L.A. Cretaceous nonmarine vertebrates of northern Eurasia. Pub. of Sankt-  
Peterburg University, Saint Petersburg. 1997. (in Russian).

Paytan, A.; Gray, E.T. Sulfur Isotopic Stratigraphy. In *The Geological Time Scale 2012*, 1st  
ed.; Gradstein, F.M., Ogg, J.G., Schmitz, M.D., Ogg, G.M., Eds.; Elsevier: Amsterdam,  
The Netherlands, 2012; Volume 1, pp. 167–180.

Paytan, A.; Yao, W.; Faul, K.L.; Gray, E.T. Sulfur Isotope Stratigraphy. In *The Geologic Time  
Scale 2020*, 1st ed.; Gradstein, F.M., Ogg, J.G., Schmitz, M.D., Ogg, G.M., Eds.;  
Elsevier: Amsterdam, The Netherlands, 2020; Volume 1, pp. 259–278.

Paytan, A.; Kastner, M.; Campbell, D.; Thiemens, M.H. Sulfur isotope composition of  
Cenozoic seawater sulfate. *Science* 1998, 282, 1459–1462.

Paytan, A.; Kastner, M.; Campbell, D.; Thiemens, M.H. Seawater sulfur isotope fluctuations  
in the cretaceous. *Science* 2004, 304, 1663–1665.

Pomazkov, K.D. (Ed.) *Kyrgyz Ssr Geological Description*; USSR Geology Publishing House  
(NEWPA): Moscow, Russia, 1972. (in Russian).

Poyarkova. Z. N. *The stratigraphy of the Cretaceous deposits of the Southern Kyrgyzstan*.  
Frunze, Ilim 1969 (book in Russian).

Redman, C., Leighton, L. Multivariate Faunal Analyses of the Turonian Bissekty Formation: Variation in the Degree of Marine Influence in Temporally and Spatially Averaged Fossil Assemblages. *PALAIOS*, 2009, Vol. 24, p. 18–26. DOI: 10.2110/palo.2007.p07-072r

Romanovskiy, G. D. Materials on the geology of Turkestan. 1878, Vol. 1. ScPb. (in Russian).

Romanovskiy, G. D. The Fergana horizon of the Cretaceous deposits and its paleontological characteristics. *Western Mineral Community*, 1882, Series 2. Part 17. (in Russian).

Romanovskiy, G. D. Materials on the geology of Turkestan. 1884, Vol. 2. ScPb. (in Russian).

Romanovskiy, G. D. Materials on the geology of Turkestan. 1890, Vol. 3. ScPb. (in Russian).

Simakov, S. N. The Cretaceous deposits of Fergana, Alay and near Alay Ranges. *Pub. VNIGRI, sp. ser.*, 1953, Vol. 5. (in Russian).

Simakov, S. N., Kleinberg, V. G., Vorobyov, A. A. Geological outlines and, oil and gas bearing deposits of the Fergana. *GovTechPub. Leningrad*, 1957.

Strauss, H. The isotopic composition of sedimentary sulfur through time. *Palaeogeogr. Palaeoclimatol. Palaeoecol.* 1997, 132, 97–118.

- Sues HD, Averianov AO. 2013 Enigmatic teeth of small theropod dinosaurs from the Upper Cretaceous (Cenomanian–Turonian) of Uzbekistan. *Can. J. Earth Sci.* 50, 306–314. (doi:10.1139/e2012-033)
- Sues HD, Averianov AO. 2014 Dromaeosauridae (Dinosauria: Theropoda) from the Bissekty Formation (Upper Cretaceous: Turonian) of Uzbekistan and the phylogenetic position of *Itemirus medullaris* Kurzanov, 1976. *Cret. Res.* 51, 225–240. (doi:10.1016/j.cretres.2014.06.007)
- Surakotra, N.; Promkotra, S.; Charusiri, P.; Maruoka, T.; Hisada, K. Sulfur, strontium, carbon, and oxygen isotopes of calcium sulfate deposits in Late Carboniferous rocks of the Loei-Wang Saphung (LWS) Area, Loei Province, Thailand. *Geosciences* 2018, 8, 229.
- Takahashi, T.; Hirahara, Y.; Miyazaki, T.; Vaglarov, B.S.; Chang, Q.; Tatsumi, Y. Precise determination of Sr isotope ratios in igneous rock samples and application to micro-analysis of plagioclase phenocrysts. *JAMSTEC Rep. Res. Dev.* 2009, 2009, 59–64.
- Tanaka, K., Anvarov, O.U.O., Zelenitsky, D.K., Ahmedshaev, A.S., Kobayashi, Y. A new carcharodontosaurian theropod dinosaur occupies apex predator niche in the early Late Cretaceous of Uzbekistan. *Royal Society Open Science* 2021, 8: 210923. <https://doi.org/10.1098/rsos.210923>.

Tang, T.; Yang, H.; Lan, X.; Yu, C.; Xue, Y.; Zhang, Y.; Hu, L.; Zhong, S.; Wei, J. Marine Late Cretaceous and Early Tertiary Stratigraphy and Petroleum Geology in Western Tarim Basin, China; China Sci. Press: Beijing, China, 1989; 141p.

Verzilin, N.N. The Cretaceous and pre-Cretaceous weathering crust of the Northern Fergana. Rep. Acad. Sci. USSR 1962, 146, 1153–1155. (in Russian).

Verzilin, N.N. The Cretaceous deposits of the northern Fergana Basin and their oil-gas bearing. Leningr. Union Nat. Exp. Res. (LNR) Geol. Mineral. Dep. 1963, 120, 35–78. (in Russian).

Vialov, O.S. The Cretaceous and Paleogene of Fergana. Ac. Sci. USSR. Tadjik-Pamir Exped. Publ. 1936, 47, 1–47. (In Russian).

Vialov, O.S. The boundary between the Cretaceous and the Paleogene at Fergana. Rep. Ac. Sci. USSR 1944, 42, 78–80. (in Russian).

Vialov, O.S. The types of the Cretaceous Sections of Fergana. Rep. Ac. Sci. USSR 1945, 49, 277–280. (in Russian).

Wakai, S.; Kawai, T.; Nagaishi, K.; Ishikawa, T. Sequential chemical separation of Sr, Nd and Pb from geological samples using multi-step extraction column chromatography. JAMSTEC Rep. Res. Dev. 2018, 27, 1–12

Zonenshain, L. P., Kuzmin, M. I. and Natapov, L. M. Geology of the USSR: A plate tectonic synthesis. AGU, Geodynamic Series, 1990, 21, 242 pp.